(12)

AFWAL-TR-81-2042

AD A113582

HIGH FRACTURE TOUGHNESS BEARING DEVELOPMENT

SKF Technology Services
SKF Industries, Inc.
King of Prussia, PA 19406

December 1981

Final Report for Period: 1 April 1979 to 30 September 1981

Approved for Public Release; Distribution Unlimited

DTIC FILE COPY

Aero Propulsion Laboratory
Air Force Wright Aeronautical Laboratories
Air Force Systems Command
Wright-Patterson Air Force Base, Ohio 45433

NOTICE

When Government drawings, specifications, or other data are used for any purpose other than in connection with a definitely related Government procurement operation, the United States Government thereby incurs no responsibility nor any obligation whatsoever; and the fact that the Government may have formulated, furnished, or in any way supplied the said drawing , specifications, or other data, is not to be regarded by implication or otherwise as in any manner licensing the holder or any other person or corporation, or conveying any rights or permission to manufacture, use, or sell any patented invention that may in any way be related thereto.

This report has been reviewed by the Office of Public Affairs (ASD/PA) and is releasable to the National Technical Information Service (NTIS). At NTIS, it will be available to the general public, including foreign nations.

This technical report has been reviewed and is approved for publication.

JAMES F. DILL
Project Engineer

HOWARD F. JONES
Chief, Lubrication Branch

FOR THE COMMANDER

ROBERT D. SHERRILL
Chief, Fuels and Lubrication Division

"If your address has changed, if you wish to be removed from our mailing list, or if the addressee is no longer employed by your organization, please notify AFWAL/POSL, W-PAFB, Ohio 45433 to help us maintain a current mailing list".

Copies of this report should not be returned unless return is required by security considerations, contractural obligations, or notice on a specific document.

AIR FORCE/56780/31 March 1982—100

DEPARTMENT OF THE AIR FORCE
AIR FORCE WRIGHT AERONAUTICAL LABORATORIES (AFSC)
WRIGHT-PATTERSON AIR FORCE BASE, OHIO 45433

REPLY TO ATTN OF: AFWAL/POSL (J. F. Dill/54347) 14 April 1982

SUBJECT: AFWAL-TR-81-2042

TO: AFWAL/TST (Stinfo)
Attn: Alsenia McFarlane

1. I have reviewed the drawings on Pages 6 and 8 of this report with the contractor SKF who wrote the report and found that the inclusion of the proprietary notice was an oversight on their part. The contractor and this office request that that statement be eliminated in any further reproduction of this report.

2. If you have any further questions on this subject, please contact me at the above extension.

James F. Dill

JAMES F. DILL
Lubrication Branch
Fuels & Lubrication Division
Aerc Propulsion Laboratory

SECURITY CLASSIFICATION OF THIS PAGE (When Data Entered)

REPORT DOCUMENTATION PAGE		READ INSTRUCTIONS BEFORE COMPLETING FORM
1. REPORT NUMBER AFWAL-TR-81-2042	2. GOVT ACCESSION NO. AD-A112	3. RECIPIENT'S CATALOG NUMBER 3582
4. TITLE (and Subtitle) HIGH FRACTURE TOUGHNESS BEARING DEVELOPMENT		5. TYPE OF REPORT & PERIOD COVERED Final Report 1 April 1979 - 30 Sept. 1981
		6. PERFORMING ORG. REPORT NUMBER AT81D016
7. AUTHOR(s) Maurer, R. E. Ninos, N. J.		8. CONTRACT OR GRANT NUMBER(s) F33615-79-C-2007
9. PERFORMING ORGANIZATION NAME AND ADDRESS SKF Industries, Inc. 1100 First Avenue King of Prussia, PA 19406		10. PROGRAM ELEMENT, PROJECT, TASK AREA & WORK UNIT NUMBERS 3048 06 07
11. CONTROLLING OFFICE NAME AND ADDRESS Aero Propulsion Laboratory (AFWAL/POSL) Air Force Wright Aeronautical Laboratories Air Force Systems Command Wright-Patterson AFB, OH 45433		12. REPORT DATE December 1981 13. NUMBER OF PAGES 61
14. MONITORING AGENCY NAME & ADDRESS (if different from Controlling Office)		15. SECURITY CLASS. (of this report) Unclassified 15a. DECLASSIFICATION/DOWNGRADING SCHEDULE

16. DISTRIBUTION STATEMENT (of this Report)

Approved for public release; distribution unlimited.

17. DISTRIBUTION STATEMENT (of the abstract entered in Block 20, if different from Report)

18. SUPPLEMENTARY NOTES

19. KEY WORDS (Continue on reverse side if necessary and identify by block number)

VIM-VAR M50 Steel
Bearing Races
High Energy Beam Heat Treatment
Fracture Toughness
Surface Transformation Hardening
Bearing Fatigue Life

20. ABSTRACT (Continue on reverse side if necessary and identify by block number)

The purpose of this program is to perform fatigue life tests to compare the rolling contact performance of high energy beam surface hardened VIM-VAR M50 steel with conventionally through hardened VIM-VAR M50 steel.

Two groups of 6009 size ball bearings (manufactured under Air Force Contract F33615-78-C-5018) were provided for life testing; one group containing conventionally through hardened VIM-VAR M50

DD FORM 1 JAN 73 1473 EDITION OF 1 NOV 65 IS OBSOLETE

SECURITY CLASSIFICATION OF THIS PAGE (When Data Entered)

steel rings, the other group containing electron beam (EB) surface hardened VIM-VAR M50 steel inner rings, and conventionally through hardened VIM-VAR M50 steel outer rings. Each group consists of twenty bearings. The inner rings for both groups were manufactured from a single heat of VIM-VAR M50 steel to eliminate possible fatigue life difference due to material factors. The outer rings for both groups were manufactured from a second single heat of VIM-VAR M50 steel.

Rolling contact fatigue life testing was performed yielding L_{10} lives of 91 x 10^6 revolutions for the conventionally through hardened bearings, and 151 x 10^6 million revolutions for the bearing group containing the EB surface hardened inner rings. These lives are consistent with the expected performance of VIM-VAR M50 steel as indicated by comparison with the calculated adjusted rating L_{10} of 62 x 10^6 revolutions.

The surface hardened bearing rings represent the first application of high energy beam heat treatment to high-speed-steel rolling bearing components. The very successful test results are significant in that they demonstrate that the traditionally high rolling contact fatigue performance of M50 steel is preserved in a surface hardened ring while improved component toughness is provided by the lower hardness subsurface material.

SUMMARY

This Final Report is submitted in accordance with the requirements of Air Force Contract F33615-79-C-2007. This report covers work performed during the period from 1 April 1979 through 30 September 1981.

The purpose of this program is to perform fatigue life tests to compare the rolling contact performance of high energy beam surface hardened VIM-VAR M50 steel with conventionally through hardened VIM-VAR M50 steel.

Two groups of 6009 size ball bearings (manufactured under Air Force Contract F33615-79-C-5018) were provided for life testing; one group containing conventionally through hardened VIM-VAR M50 steel rings, the other group containing electron beam (EB) surface hardened VIM-VAR M50 steel inner rings, and conventionally through hardened VIM-VAR M50 steel outer rings. Each group consists of twenty bearings. The inner rings for both groups were manufactured from a single heat of VIM-VAR M50 steel to eliminate possible fatigue life differences due to material factors. The outer rings for both groups were manufactured from a second single heat of VIM-VAR M50 steel.

Rolling contact fatigue life testing of conventionally through hardened VIM-VAR M50 steel bearings was conducted to provide a baseline against which the surface hardened M50 bearing performance is compared. The through hardened inner ring L_{10} life obtained is 91×10^6 revolutions. This life is consistent

with the expected performance of VIM-VAR M50 steel, as indicated by comparison with the calculated inner ring adjusted rating L_{10} life of 62×10^6 revolutions.

Early failures were experienced in the testing of the first few bearings containing surface hardened rings. Metallurgical analysis revealed the presence of series of micro-pits aligned in the cross-groove direction in the ball paths of both tested and untested inner rings. The origin of these pits was traced to a near surface microstructural alteration associated with excessive surface temperature experienced during EB hardening. The pits were formed through interaction of this microstructural alteration with the ball path grinding operation. These pits represent a severe disruption of the integrity of the rolling contact surface. The extremely early failures experienced are consistent with their presence.

The EB hardened inner rings were reground to remove the life limiting surface condition and assembled into bearings. Rolling contact fatigue testing provided an impressive L_{10} life of 151×10^6 revolutions. These surface hardened bearing rings represent the first application of high energy beam heat treatment to high-speed-steel rolling bearing components. The very successful test results are significant in that they demonstrate that the traditionally high rolling contact fatigue performance of M50 steel is preserved in a surface hardened ring, while

improved component toughness is provided by the lower hardness subsurface material.

TABLE OF CONTENTS

ILLUSTRATIONS

ILLUSTRATIONS (CONTINUED)

TABLES

PREFACE

This Final Report documents work performed under Air Force Contract F33615-79-C-2007, "High Energy Toughness Bearing Development," during the period 1 April 1979 through 30 September 1981.

The contract with SKF Industries, Inc., King of Prussia, Pennsylvania, was initiated to provide testing and subsequent analysis of bearings manufactured under a separate AFWAL Manufacturing Technology Program (Air Force Contract F33615-78-C-5018). This testing was performed under the direction of Dr. James F. Dill, AFWAL/POSL, Wright-Patterson Air Force Base, Ohio.

Work on the contract was performed at SKF Industries, Inc., King of Prussia, Pennsylvania under Mr. J. H. Johnson, Director of Development, by Mr. R. E. Maurer, Project Leader, Mr. F. R. Morrison, Supervisor, Mechanical Laboratories, and Mr. N. J. Ninos, Senior Test Engineer.

This report is published for information only and does not necessarily represent the recommendations, conclusions, or approval of the Air Force.

HIGH FRACTURE TOUGHNESS BEARING DEVELOPMENT

INTRODUCTION

One of the factors limiting the use of rolling element bearings to below 2.5 million DN is the fracture toughness of the M50 steel commonly used in aircraft turbine engine mainshaft bearings. Testing [1,2]* has shown that while ball bearings can be designed to operate successfully at 3 million DN (from a stability and lubrication standpoint) they can suffer catastrophic ring fracture that may or may not be in conjunction with surface spalling. The hoop stress associated with high DN operation affects crack initiation and/or propagation behavior in such a way as to promote radial ring fracture.

High speed tool steels, such as M50, are conventionally through hardened to obtain the required hardness and microstructural characteristics for maximum rolling contact performance. The resulting high hardness and high strength are at the opposite end of the mechanical properties spectrum from high toughness in these material systems. An existing AFWAL, Manufacturing Technology program (Contract F33615-78-C-5018) is underway to establish manufacturing processes whereby M50 steel bearing races can be selectively surface hardened using a high energy beam. Since only a relatively shallow layer of high hardness surface material is required to support rolling contact stressing,

* Numbers in brackets refer to references listed on Page 56.

the bulk of an aircraft bearing race can be independently processed to provide hardness (toughness) consistent with the bulk stress environment. Subsequently, the rolling contact surface can be selectively hardened with a high energy beam to provide the required layer of high hardness material. The resulting structural combination provides high surface hardness to support rolling contact stresses, and high core toughness to inhibit through section crack propagation.

Within the AFWAL Manufacturing Technology program, two groups of 6009 size ball bearings have been produced; a bearing group containing conventionally through hardened M50 steel inner and outer races, and a bearing group containing conventionally through hardened M50 steel outer rings and high energy beam surface hardened, M50 steel inner rings.

The purpose of this program is to determine the rolling contact fatigue life of the bearings manufactured in the Manufacturing Technology program, and to assess the relative fracture behavior of conventionally through hardened and surface hardened M50 steel bearing races.

TECHNICAL APPROACH

This program consists of three tasks:

Task I	-	Fatigue Life Testing
Task II	-	Radial Expansion Testing
Task III	-	Failure Analysis

Task I involves rolling contact endurance testing of two groups, each containing twenty 6009 size deep groove ball bearings. One bearing group represents conventionally through hardened M50 steel, and the other represents high energy beam surface hardened M50 steel.

The radial expansion testing of Task II is to assess the relative fracture behavior of conventionally through hardened and high energy beam surface hardened bearing rings made of M50 steel. In these tests, the inner rings of the bearings which have completed endurance testing were expended on a tapered mandrel until they fractured.

Failure analysis of the endurance tested bearings and characterization of inner rings fractured by radial expansion comprises Task III.

PROCEDURAL DETAILS

Two groups of 6009 size deep groove ball bearings were manufactured under AFWAL Manufacturing Technology Contract F33615-78-C-5018. Twenty 6009 VCC bearings were produced with conventionally heat treated (through hardened) VIM-VAR M50 steel inner and outer rings and balls. Figure 1 is the 6009 VCC assembly drawing. Table 1 contains ring material heat identification, analysis and processing information.

A second group of twenty bearings, designated 6009 VCD, was manufactured with electron beam (EB) surface hardened VIM-VAR M50 steel inner rings and conventionally through hardened VIM-VAR M50 steel outer rings. Figure 2 is the 6009 VCD assembly drawing. Dimensionally, the VCC and VCD bearings are identical. The only difference (aside from inner ring heat treat processing) is in the fit grinding to match inner and outer rings to provide the required internal clearance in the assembled bearing. Generally, the fit grinding is performed with the inner rings, and this procedure was followed with the through hardened group. Since it was desired to closely control the stock removal from the EB surface hardened rings, fit grinding of the outer rings was performed. Table 2 contains EB processing information and ring characterization.

The inner rings for both groups were made from a single

6009 VCC	
VENDOR'S PART Nº	6009 VCC
VENDOR'S DRAWING Nº	6009 VCC
BEARING TOLERANCE	ABEC 5
Nº & SIZE OF BALLS	13 - 11/32" DIA
INTERNAL RADIAL LOOSENESS (UNDER 11 LB GAGE LOAD)	0002" - 0009"
MAX (REF) END PLAY (UNDER 11 LB GAGE LOAD)	008"
DESIGN CONTACT ANGLE	RADIAL
CAGE WIDTH (MAX. OVER RIVETS)	.580"
PITCH DIA (REF.)	2.363"

1. OUTER RING TO BE MADE FROM VIM VAR M50 ST'L., THROUGH HARDENED, HARDNESS Rc 50 MIN
2. INNER RING TO BE MADE FROM VIM VAR M50 ST'L., THROUGH HARDENED, HARDNESS Rc 60 MIN
3. BALLS TO BE MADE FROM VIM VAR M50 ST'L., THROUGH HARDENED. HARDNESS Rc 60 MIN
4. CAGE TO BE MADE FROM AMS 6414 ST'L., TWO PIECE MACHINED AND RIVETED INNER LAND RIDING HARDNESS Rc 28-35.
5. CAGE TO BE SILVER PLATED ALL OVER .001"-.002" PER SURFACE PER AMS 2412. BAKE AT 475°-500°F FOR 2 HRS. DIMS SHOWN ARE AFTER PLATING.
6. CAGE TO BE 100% FLUORESCENT PENETRANT INSPECTED.
7. 100% VISUAL INSPECTION.
8. RIVET TO BE MADE FROM AMS 7225 MATERIAL.
9. BRG. TO BE PERMANENTLY MARKED WITH CUST PART Nº. & LATEST CHANGE LETTER

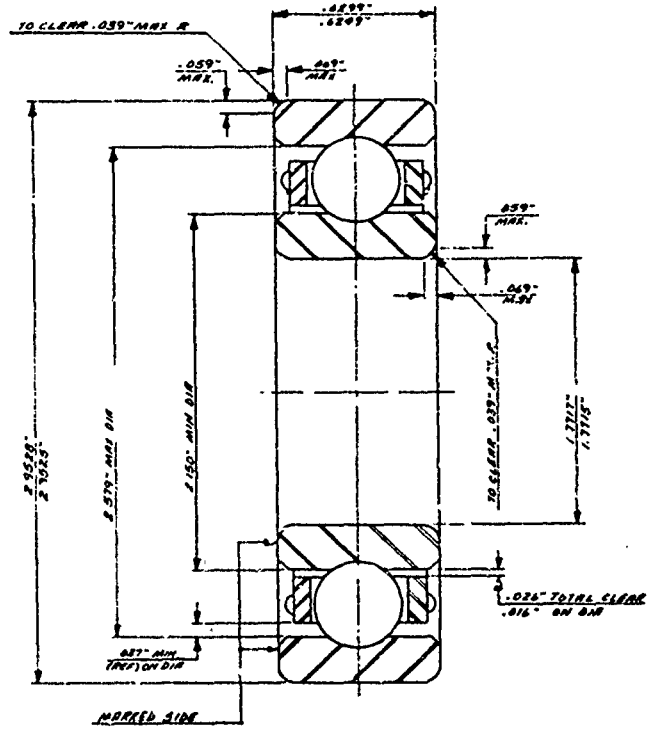

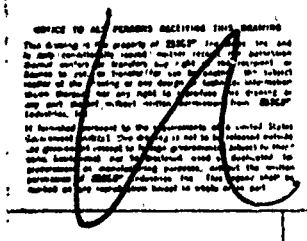

SKF INDUSTRIES, INC. PHILADELPHIA, PA.	BEARING NO 6009 VCC	DRAW PMS	CHECK	APPR	SCALE C/S	DATE 5-5-81
						6009 VCC

Figure 1. Assembly Drawing for 6009VCC - Through Hardened M50 Steel Test Bearing

TABLE 1

MATERIAL AND PROCESSING INFORMATION FOR THROUGH HARDENED BASELINE TEST BEARINGS

BEARING TYPE: 6009 VCC BALL BEARING

MATERIAL:

Inner Ring: VIM-VAR M50 steel, extruded hollow bar, 2.3130" OD x 0.3590" wall

Outer Ring: VIM-VAR M50 steel, extruded hollow bar, 3.171" OD x 0.406" wall

Composition:

	C	Mn	P	S	Si	Cr	Ni	Mo	V
Inner Ring	.84	.29	.007	.004	.20	4.17	.01	4.24	.98
Outer Ring	.84	.27	.009	.004	.19	4.11	.01	4.27	.98
Specified	.8/.85	.15/.35	.015max	.01max	.1/.25	4/4.25	.1max	4/4.5	.9/1.1

HEAT TREATMENT: As per SKF Process Specification 471020.
Specified hardness - 60 - 63 RC
Measured hardness - 61.5 RC (inner and outer rings)
Retained austenite determined to be less than 1%.

SURFACE FINISH: Average of three cross-groove readings per ring on a five ring sample. Individual readings not to exceed 12 microinch "AA". Measurements made after etch inspection for grinding damage. Bearings assembled in etched condition.

Inner rings: 6.7 microinch "AA"

Outer rings: 9.5 microinch "AA"

BALLS: Grade 10, VIM-VAR M50, 11/32" diameter
13 balls per bearing
Measured hardness - RC 62.5

6009 VCD

VENDOR'S PART Nº	6009 VCD
VENDOR'S DRAWING Nº	6009 VCD
BEARING TOLERANCE	ABEC 5
Nº & SIZE OF BALLS	13 - 11/32" DIA
INTERNAL RADIAL LOOSENESS (UNDER 11 LB GAGE LOAD)	.0002"- 0009"
MAX (REF) END PLAY (UNDER 11 LB GAGE LOAD)	008"
DESIGN CONTACT ANGLE	RADIAL
CAGE WIDTH (MAX OVER RIVETS)	.580"
PITCH DIA (REF)	2.363"

1. OUTER RING TO BE MADE FROM VIM VAR M50 ST'L., THROUGH HARDENED, HARDNESS Rc 60 MIN
2. INNER RING TO BE MADE FROM VIM VAR M50 ST'L , ELECTRON BEAM SURFACE HARDENED, HARDNESS Rc 60 MIN
3. BALLS TO BE MADE FROM VIM VAR M50 ST'L., THROUGH HARDENED, HARDNESS Rc 60 MIN.
4. CAGE TO BE MADE FROM AMS 6414 ST'L , TWO PIECE MACHINED AND RIVETED INNER LAND RIDING HARDNESS Rc 28 - 35.
5. CAGE TO BE SILVER PLATED ALL OVER 001"- 002" PER SURFACE PER AMS 2412. BAKE AT 475°-500° F. FOR 2 HRS DIMS. SHOWN ARE AFTER PLATING.
6. CAGE TO BE 100% FLUORESCENT PENETRANT INSPECTED.
7. 100% VISUAL INSPECTION.
8. RIVET TO BE MADE FROM AMS 7225 MATERIAL.

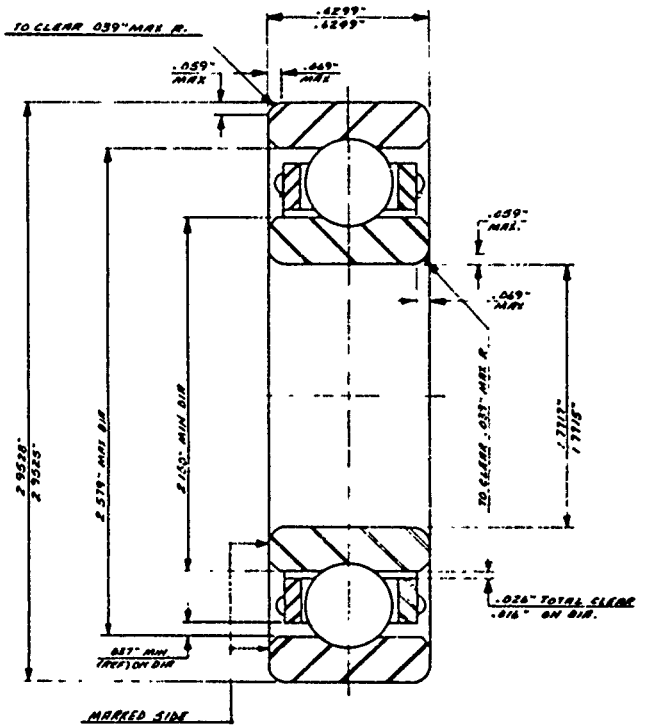

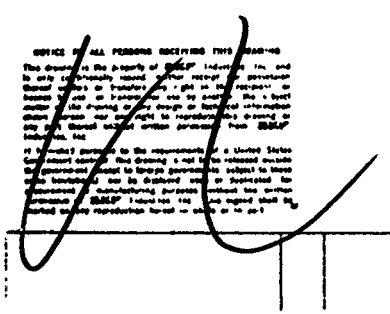

SKF INDUSTRIES, INC. PHILADELPHIA, PA.

BEARING Nº 6009 VCD

DRAWN	CHECK	APPR	SCALE 2/1	2X
PMP	WJH	DK	DATE 5 5 N	

6009 VCD

Figure 2. Assembly Drawing for 6009VCD EB Hardened M50 Steel Test Bearing

TABLE 2

MATERIAL AND PROCESSING INFORMATION FOR
ELECTON BEAM HARDENED TEST BEARINGS

BEARING TYPE: 6009 VCD BALL BEARING

MATERIAL: Inner ring and outer ring material same as for through hardened baseline bearings (TABLE I)

HEAT TREATMENT: Outer Ring:

Through hardened as per SKF Process Specification 471020.
Specified hardness - 60-63 RC
Measured hardness - 61.5 RC
Retained austenite - less than 1%

Inner Ring:

Inner rings were processed through the following thermal treatment:

1. Through hardened as per SKF Process Specification 471020.
2. Tempered at 1350°F (732°C) for two hours to provide hardness of 35 RC.
3. Ball path surface subsequently EB hardened in one revolution scan pass with a profiled EB raster pattern (beam power: 6 kw, scan rate: 38 ipm)
4. Double tempered at 1025°F (550°C) for three hours.

Case depth: 0.020-0.025 inch (to 50 RC)
Surface hardness: 61.5-62.5 RC

SURFACE FINISH: Average of three cross-groove readings per ring on a five ring sample. Individual readings not to exceed 12 microinch "AA". Measurements made after etch inspection for grinding damage.

Inner rings: 6.8 microinch "AA"
Outer rings: 9.5 microinch "AA"

BALLS: Grade 10, VIM-VAR M50, 11/32" diameter
13 balls per bearing
Measured hardness - RC 62.5

heat of VIM-VAR M50 steel. A second heat of VIM-VAR M50 was used for the outer rings of both bearing groups.

TASK I - Fatigue Life Testing

Test Equipment

Life testing was conducted on SKF R-2 endurance test machines. The R-2 test machine is schematically depicted in Figure 3. Basically, this machine consists of a horizontal arbor of symmetrical configuration, which is supported on both sides of its center by two cylindrical roller bearings located in pillow blocks on a cast machine base. The test bearings are located on each end of the arbor in independent housings to minimize interaction between the test specimens. Loading is radially applied by means of a dead weight and lever arrangement. A centrally located pulley on the arbor rotates the inner rings at the desired speed.

The test bearing operating temperature is measured with a thermocouple contacting the outer ring. A test floor control system incorporating a Data General Nova 800 computer, as a central processing unit, monitors the thermocouple output.

Bearing failures are detected by a vibration sensitive transducer (Vibraswitch) which is set at the beginning of each test run. The Vibraswitch stops the test machine when the general vibration level increases significantly over the initial

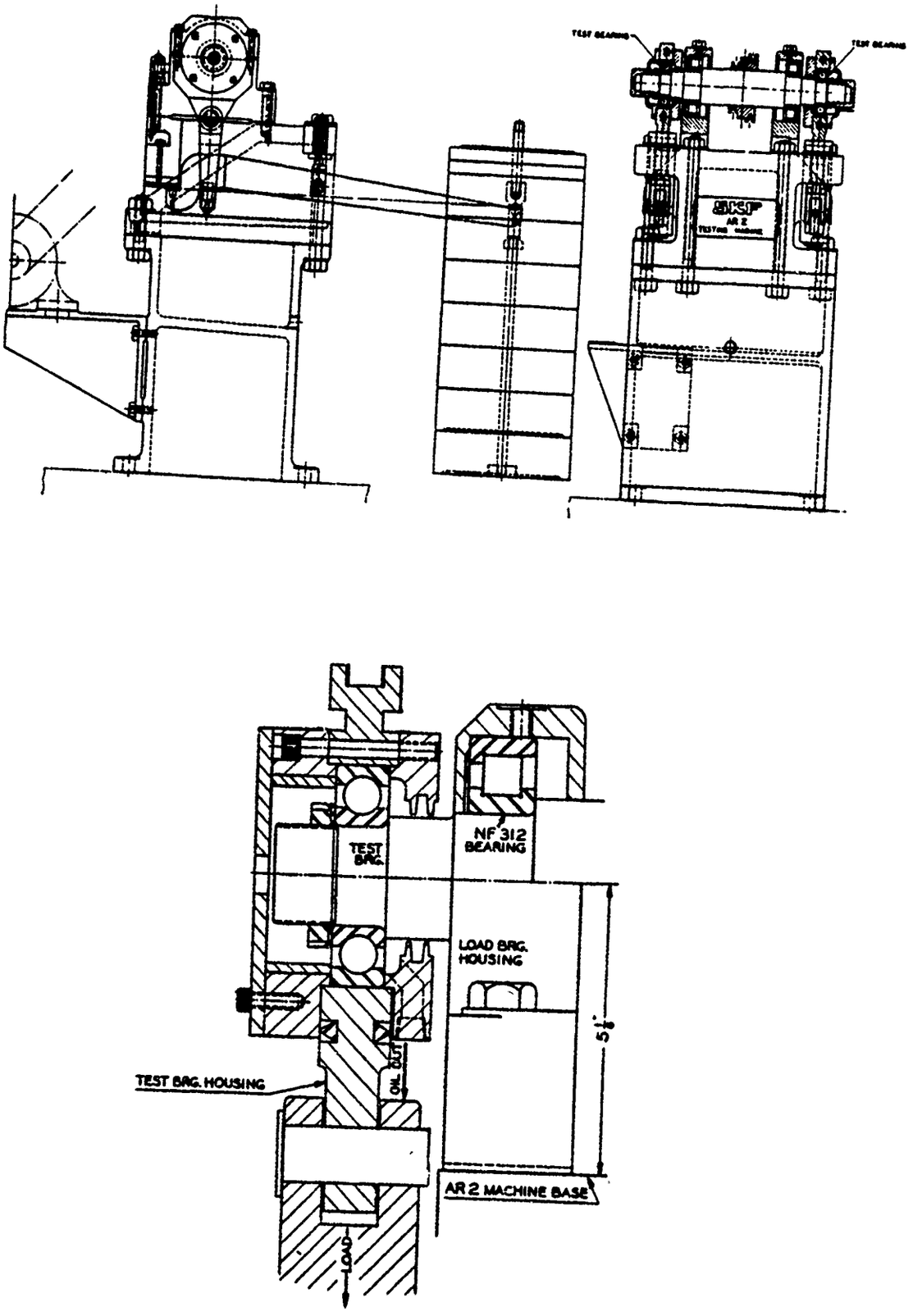

Figure 3. R2 Type Bearing Test Machine

setting; a condition indicative of a spall on a bearing component.

Test bearings were lubricated from a common oil supply system containing synthetic lubricating fluid conforming to MIL-L-7808G. A sufficient quantity of oil was supplied to assure adequate lubrication and to control the bearing operating temperature.

Endurance Test Procedure

Prior to use, the anti-rust preservative was removed from each test bearing by washing with a solvent. To facilitate mounting of the test bearings on the test machine arbor, the bearings were heated in an oven to 135°C (408°K). When cool the interference fit was 0.0006 to 0.0012 inch (0.015 to 0.030mm). The clearance between the outer rings and the housings ranged from 0.0004 to 0.002 inch (0.010 to 0.050mm).

The bearings were tested under a radial force of 1685 lbf. (7.5kN) at a speed of 9700 rpm (1016 rad/sec), and an operating temperature of 60°C (333°K). A synthetic diester lubricant conforming to MIL-L-7808G was circulated at a rate to control bearing operating temperature to within $\pm$ 5°C.

All bearings were run to failure or to an established time up life of 500 million revolutions.

At the conclusion of a test run, each bearing was disassembled and examined to determine the condition of the components

and mode of failure.

TASK II - Radial Expansion Testing

Inner rings from the endurance tested bearings were pressed over a tapered mandrel, and the travel distance at the point of ring fracture was recorded. The apparatus for this testing is illustrated in Figure 4.

The mandrel taper is 0.0015 inch increase in diameter per inch of length over 25 inches (1.5 microns per millimeter over 630 millimeters). A thin coating of molybdenum disulfide was applied to the mandrel to prevent galling of the mandrel and inner ring contacting surfaces. Testing was performed on a Baldwin Lima Hamilton Universal Testing Machine.

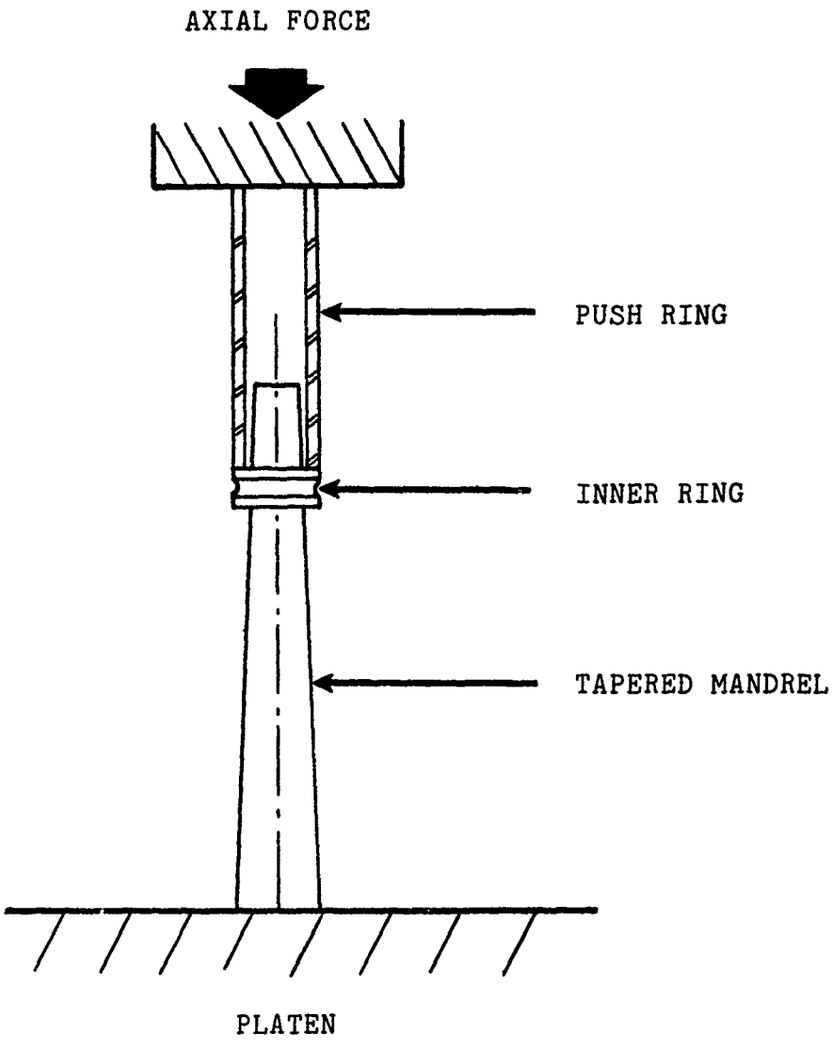

Figure 4. Apparatus for Radial Expansion of Bearing Inner Rings

RESULTS

Bearing Life Tests

Conventionally Through Hardened M50 Steel Baseline

The results of the life testing of the conventionally through hardened VIM-VAR M50 steel bearing group are presented in Table 3. Fifteen failures were produced, distributed as follows: seven inner ring, five outer ring, one combination inner and outer ring and two bearings in which balls failed. The frequency of outer ring failure is unusual, since theoretically the outer ring life should be approximately four times that of the inner ring. Furthermore, the outer ring lives are noted to be less than that expected from VIM-VAR M50 steel.

The outer rings of these bearings were made from a different heat of steel than that used for the inner rings. The outer ring heat complies with SKF material acceptance specifications and there is no evidence that material defects initiated the outer ring failures. The mechanical factors involved in the test procedure were reviewed to determine possible sources for results biasing. No mechanical or procedural irregularities or deficiencies were identified.

Standard Weibull statistical techniques are capable of estimating the experimental lives of individual bearing components. Given the apparent poor performance of the outer ring material, and that the electron beam surface hardening was applied only to the inner rings of the experimental bearing group, it is

TABLE 3

TEST RESULT DETAILS

6009 VCC Ball Bearing Endurance Test

Material: VIM-VAR AISI M50 Tool Steel

Test Elements: Inner Ring - Conventionally Through Hardened

Test Conditions: Inner Ring Speed - 9700 rpm
Applied Load - 7.495 kN (1685 lbf)

Lubricant: MIL-L-7808G

Bearing No.	Life Million Revs.	Failure Mode
104	475	Inner ring spall
105	813	Inner ring spall
106	175	Inner ring spall
107	110S	Outer ring spall
108	111	Inner & Outer rings spall
109	73S	Outer ring spall
110	564S	Susp. OK Time Up
112	174S	Outer ring spall
113	46	Inner ring spall
114	515S	Susp. OK Time Up
115	274S	4 balls spalled
116	94S	Outer ring spall
117	133S	Susp. OK (noisy)
119	886S	Susp. Time Up
120	73	Inner ring spall
121	133	Inner ring spall
122	111S	Outer ring spall
123	169S	2 balls spalled
124	714S	Susp. Time Up
128	351S	Susp. rough
129	468	Inner ring spall

Inner Ring Adjusted Rating L_{10} Life = 62×10^6 revolutions

Inner Ring Experimental L_{10} Life = 91×10^6 revolutions

L_{10} Lower Confidence Limit = 17.4×10^6 revolutions

L_{10} Upper Confidence Limit = 171×10^6 revolutions

Slope = 1.134

appropriate to compare fatigue life on the basis of inner ring performance.

The experimental L_{10} life was calculated using a maximum likelihood statistical method [3] for the inner rings only. Other modes of failure (i.e. outer rings or balls) were treated as suspensions in the analysis. Accordingly, the experimental inner ring L_{10} life is 91×10^6 revolutions.

The calculated adjusted rating L_{10} life (Appendix A) is 62×10^6 revolutions, which is less than the experimental L_{10} life of 91×10^6 revolutions. This comparison indicates inner ring fatigue performance consistent with what is expected for VIM-VAR M50 steel. With the confidence limits on the experimental estimate, the difference between the experimental L_{10} and adjusted rating life is not statistically significant.

Electron Beam Surface Hardened M50 Steel

Extremely early failures were experienced with the first three test bearings containing EB processed inner rings. Spalling failure occurred as early as 1.8×10^6 revolutions. With the baseline bearings, the earliest failure was after 46×10^6 revolutions.

Metallurgical analysis of the early failures revealed the nature and extent of a microstructural deficiency in the surface and near surface region of the EB processed inner rings. This

is described in detail in the Discussion section of this report. The EB processed inner rings were reground to remove this surface condition. The rings were assembled into bearings and life tested under the same conditions as the through hardened baseline bearing group. The test results are contained in Table 4.

Seven failures were experienced with the twenty bearing group: six inner ring failures and one failure involving a single ball. The remaining thirteen bearings completed the time-up of 859 hours (500×10^6 revolutions) without failure. Inner ring L_{10} life was calculated using the maximum likelihood statistical method employed for the baseline group, treating the bearing failure involving a ball as a suspension. The experimental L_{10} life for the EB processed inner rings is 151×10^6 revolutions.

Weibull plots for both bearing groups are presented in Figure 5. Nelson's cumulative hazard method [4] was used to compute the cumulative failure percentages for the test points shown on Figure 5. The Weibull plot corresponds to the L_{10} and L_{50} estimates provided by the maximum likelihood method employed [3]. Good fit of the points to the Weibull distribution is exhibited with the through hardened baseline data. Somewhat less fit is exhibited by the points and Weibull plot for the EB surface hardened test data. The latter is primarily attributed to the fact that EB processed inner ring failures all occurred at the circumferential location corresponding to start-stop

TABLE 4

TEST RESULT DETAILS

6009 VCD BALL BEARING ENDURANCE TEST

Material: VIM-VAR AISI M50 Tool Steel

Test Elements: Inner Ring - Electron Beam Surface Hardened

Test Conditions: Inner Ring Speed - 1016 rad/s (9,700 rpm)
Applied Load - 7.495 kN (1685 lbf)

Lubricant: MIL-L-7808G

Bearing No.	Life Million Revs.	Failure Mode
229	500	Susp. O.K. - Time Up
230	500	Susp. O.K. - Time Up
231	560	Susp. O.K. - Time Up
232	137	Inner Ring Spall
234	500	Susp. O.K. - Time Up
236	500	Susp. O.K. - Time Up
237	500	Susp. O.K. - Time Up
238	505	Susp. O.K. - Time Up
243	190	Inner Ring Spall
245	506	Susp. O.K. - Time Up
246	500	Susp. O.K. - Time Up
247	196	Inner Ring Spall
249	153	Inner Ring Spall
250	325	Inner Ring Spall
251	224	Inner Ring Spall
252	509	Susp. O.K. - Time Up
233	500	Susp. O.K. - Time Up
239	550	Susp. O.K. - Time Up
253	72	Susp. (1 ball failed)
225	500	Susp. O.K. - Time Up

Inner Ring Adjusted Rating L_{10} Life = 62×10^6 revolutions

Inner Ring Experimental L_{10} Life = 151×10^6 revolutions

L_{10} Lower Confidence Limit = 23.4×10^6 revolutions

L_{10} Upper Confidence Limit = 281×10^6 revolutions

Slope = 1.287

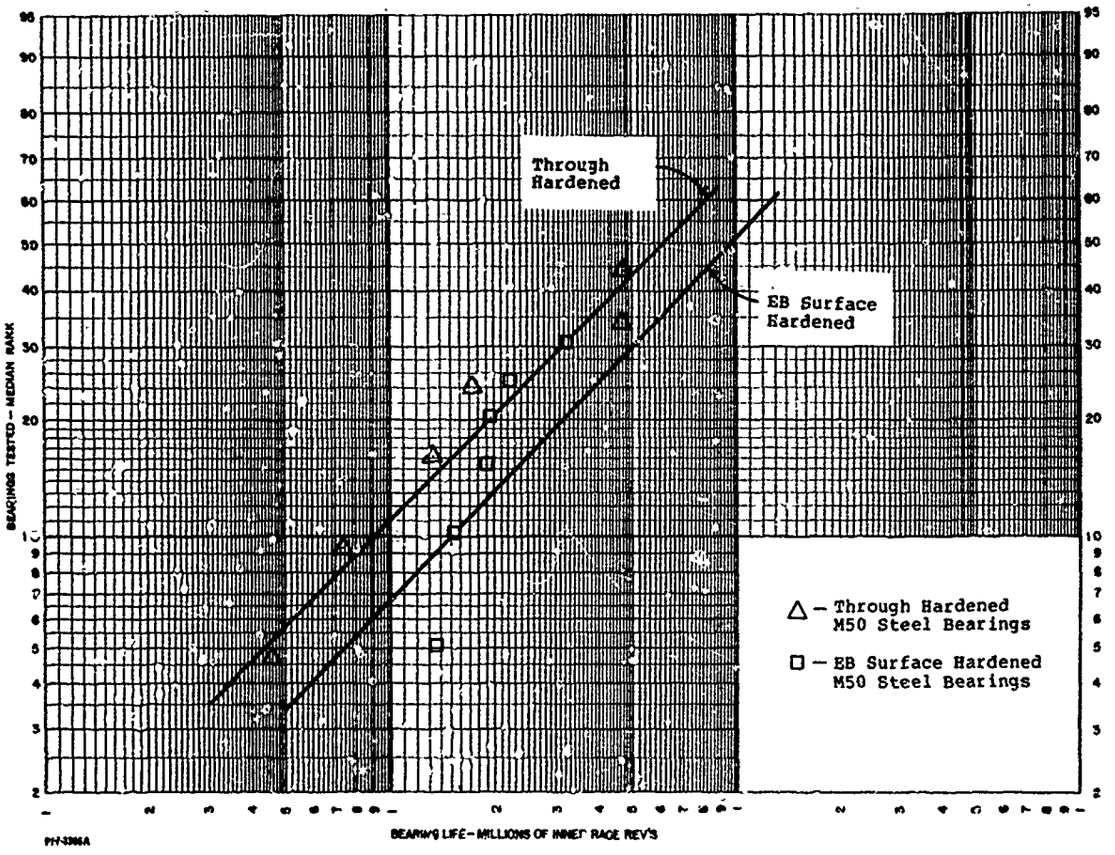

Figure 5. Weibull Plots of Through Hardened and EB Surface Hardened M50 Steel Bearing Life Data

juncture of the EB heating pass. Additionally, with maximum likelihood method used, the very high percentage of time-up bearings is more heavily weighted.

Radial Expansion Tests

Inner rings from the endurance tested bearings were pressed up a tapered mandrel to fracture. Hoop stress was calculated as described in Appendix B. Calculated hoop stress, diametral expansion and ring condition (i.e. spalled or not spalled) are listed in Table 5.

Through hardened ring fractures were fragmentary, producing several pieces. If a ring contained a surface spall, fracture during radial expansion appears to have originated at the spall initiation point. All spalled rings fractured at lower values of calculated hoop stress than rings not containing spalls. Photographs of typical fractures are shown in Figures 6 and 7.

EB surface hardened rings exhibited singular through section fractures; i.e. no fragmentation was experienced. Macro-characteristics of fractured rings are presented in Figures 8 and 9.

TABLE 5

RING EXPANSION DATA

Inner Ring Identification Number	Heat Treatment	Ring Condition	Diametral Expansion Inch	Diametral Expansion (μm)	Calculated Hoop Stress KSI	Calculated Hoop Stress (MPa)
106	Through Hardened	Spalled	.0129	(330)	187	(1280)
124	Through Hardened	Spalled	.0131	(338)	191	(1320)
108	Through Hardened	Spalled	.0140	(356)	201	(1390)
113	Through Hardened	Spalled	.0158	(401)	226	(1560)
120	Through Hardened	Spalled	.0165	(419)	236	(1640)
253	EB Surface Hardened	Not Spalled	.019?	(488)	276	(1902)**
247	EB Surface Hardened	Spalled	.0194	(493)	278	(1922)**
105	Through Hardened	Spalled	.0221	(561)	317	(2180)
109	Through Hardened	Not Spalled	.0221	(561)	317	(2180)
107	Through Hardened	Not Spalled	.0235	(597)	338	(2320)**
116	Through Hardened	Not Spalled	.0238	(605)	342	(2350)**
117	Through Hardened	Not Spalled	.0238	(605)	342	(2350)**
122 *	Through Hardened	Not Spalled	.0238	(605)	342	(2350)**
115 *	Through Hardened	Not Spalled	.0245	(622)	351	(2420)**
128 *	Through Hardened	Not Spalled	.0245	(622)	351	(2420)**
123 *	Through Hardened	Not Spalled	.0249	(632)	356	(2460)**
112	Through Hardened	Not Spalled	.0252	(640)	362	(2500)**

* - Ring did not fracture

** - Calculated hoop stress assumes elastic behavior. These values exceed published yield strengths. Core material of EB processed rings (RC35) - Y.S. = 170 ksi. Through hardened material (RC61.5) - Y.S. = 330 ksi.

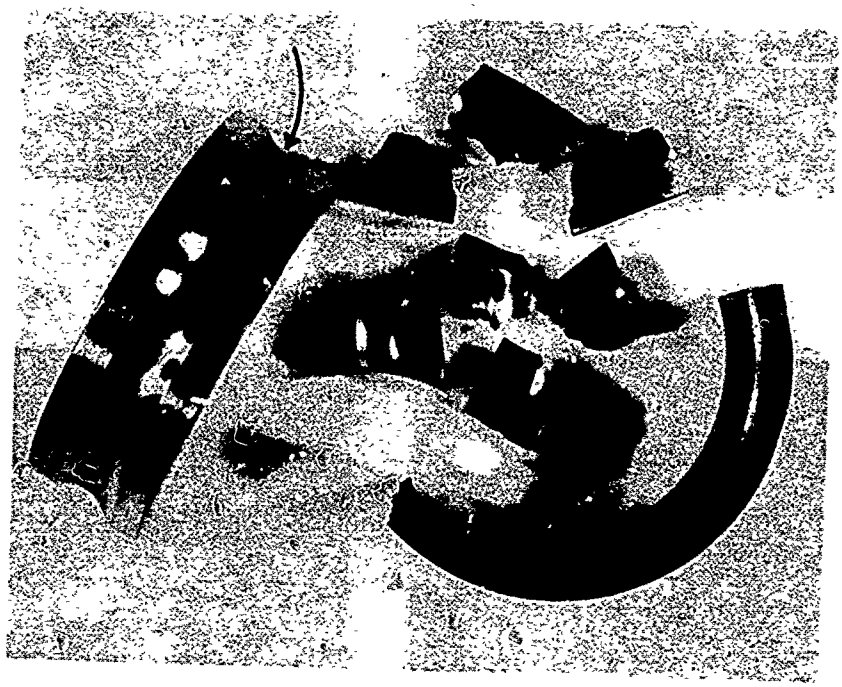

Figure 6. Characteristic Fragmentary Fracture of Through Hardened M50 Steel Inner Ring Resulting from Radial Expansion. Primary Fracture Through Spall at Arrow. (Bearing #105)

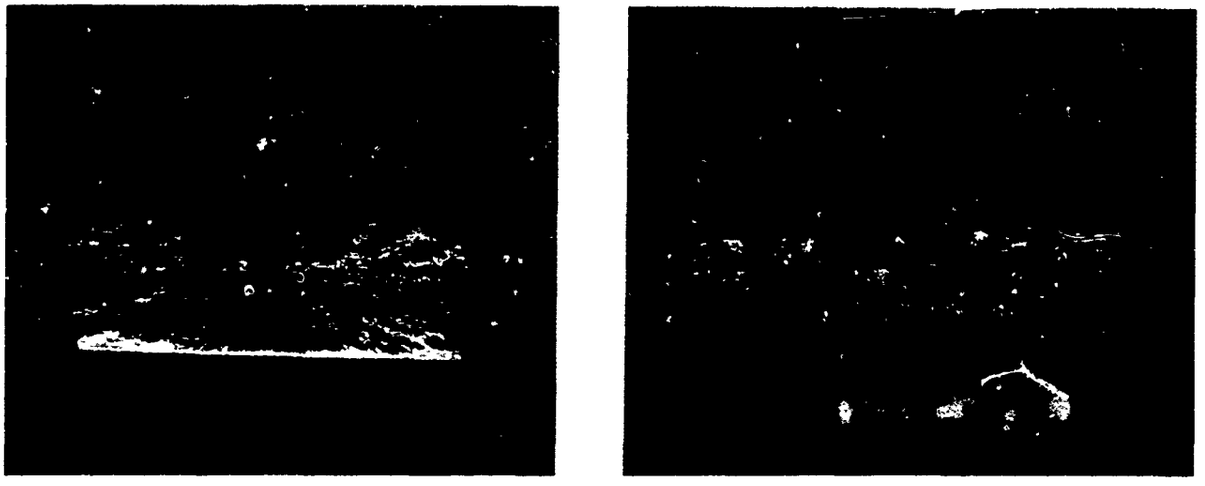

Bearing #120

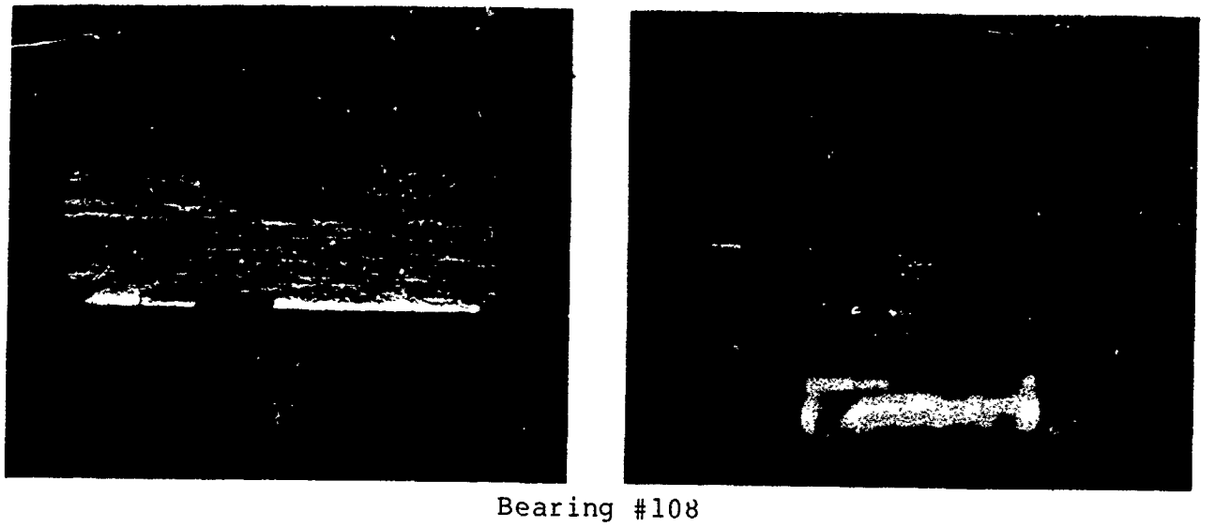

Bearing #108

Figure 7. Fracture Surfaces of Radially Expanded Through Hardened M50 Steel Inner Rings Showing Fracture Initiation at Spall (4X)

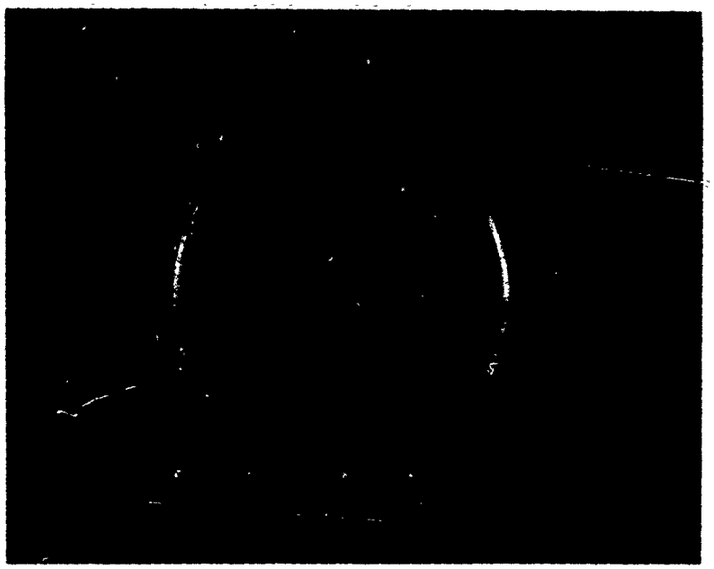

(1X)

Figure 8. Characteristic Fracture of EB Surface Hardened M50 Steel Inner Ring Resulting from Radial Expansion

A

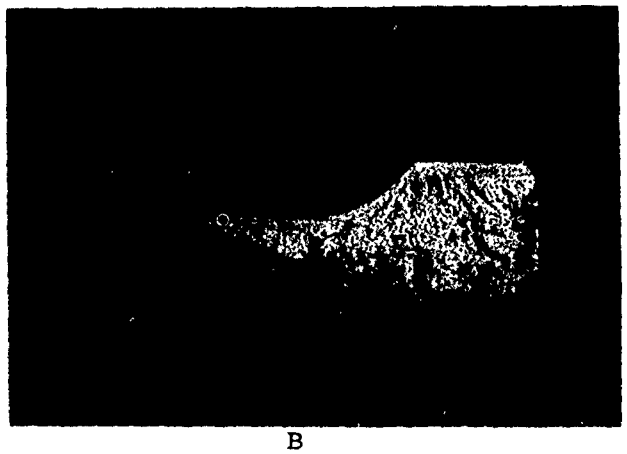

B

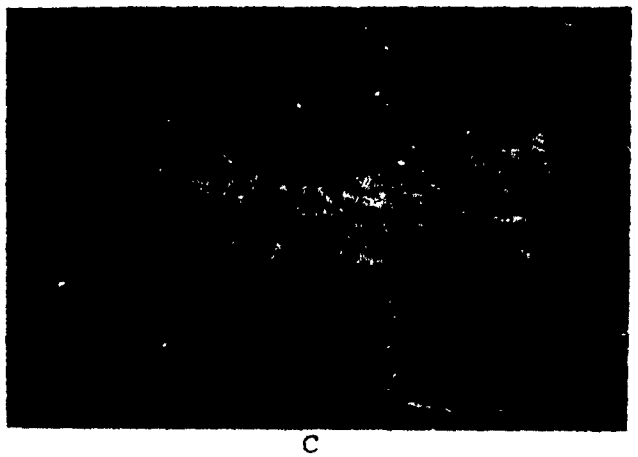

C

Figure 9. Fracture Surfaces of Radially Expanded EB Surface Hardened M50 Steel Inner Rings
(A) Bearing #253 - EB Hardening Pattern Highlighted by Variations in Fracture Mode
(B) Bearing #253 - Fracture Initiation from Ball Path-Land Juncture
(C) Bearing #247 - Fracture Initiation from Spall in Bottom of Ball Groove

(4X)

DISCUSSION

Failure Analysis - Through Hardened M50 Steel Baseline Bearings

Inner ring failures in the M50 steel baseline group exhibit classical subsurface initiated rolling contact fatigue spalls. There are no indications of surface distress associated with marginal lubrication conditions. There are no indications of spall initiating surface defects associated with these failures (e.g. grinding furrows, dents, residual machining lines, etc.), or of the presence of nonmetallic inclusions.

Hardness and microstructural characteristics consistent with production process specifications were reconfirmed. Figure 10 contains a photomicrograph showing typical microstructural appearance.

Outer ring failure frequency was greater than what would be predicted under the test conditions, however, no indications of mechanical or metallurgical deficiencies are apparent. Since only one of the inner ring failures was associated with outer ring failure, statistical analysis of independent inner ring fatigue performance was made.

Failure Analysis - Electron Beam Surface Hardened M50 Steel Inner Rings

Two 6009 VCD bearings containing electron beam (EB) surface

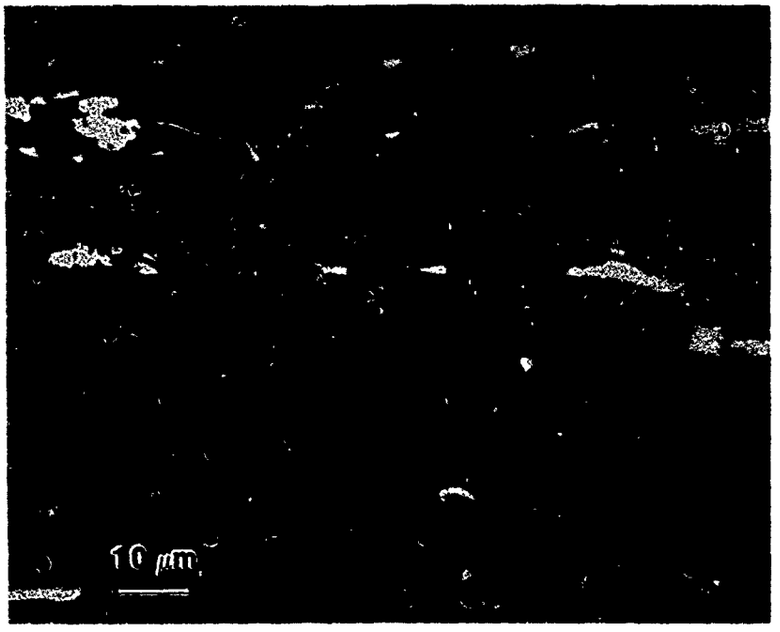

Figure 10. Microstructure of Conventionally Through Hardened M50 Steel Bearings (Nital Etch)

hardened M50 steel inner rings exhibited inner ring spalling after only five hours of testing (3×10^6 revolutions). Two additional bearings containing EB processed inner rings were put on test, and one of these spalled after three hours (1.8×10^6 revolutions).

Figure 11 is a scanning electron micrograph of the spall in the inner ring ball groove of one of the bearings tested for five hours. Circumferentially oriented texturing (i.e. grinding lay) of the ball groove surface is characteristic of ring manufacturing procedures. Unusual cross-groove indications, superimposed on the circumferential texture, are clearly indicated on the surface surrounding the spall in Figure 11. This pattern of circumferential and cross-groove texturing was observed on all of the EB processed rings and covered 360° in the bottom of the ball groove.

Presented in Figure 12 is a series of scanning electron micrographs which highlights the topographic features giving rise to this unusual surface texture. The individual cross-groove indications are shown to consist of aligned micro-pits.

Figure 13 is a similar series of micrographs of the surface of the second ring that was tested for five hours. The same pattern of aligned cross-groove micro-pits is observed.

A bearing that had not been tested was disassembled and the inner ring examined. Figure 14 shows that the cross-groove

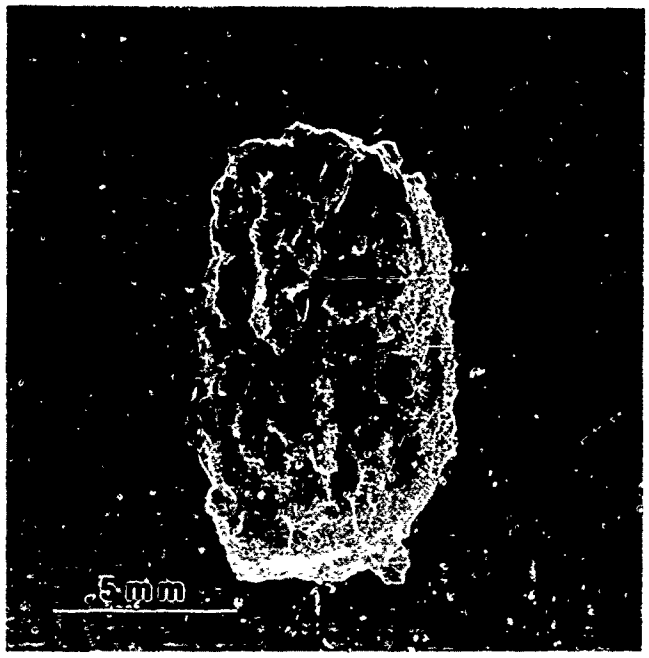

Circumferential
Direction

Figure 11. SEM Micrograph Showing Cross-Groove and Circumferential Texturing, and Spall Produced After Five Hours of Testing in EB Hardened Inner Ring (Bearing #331-201)

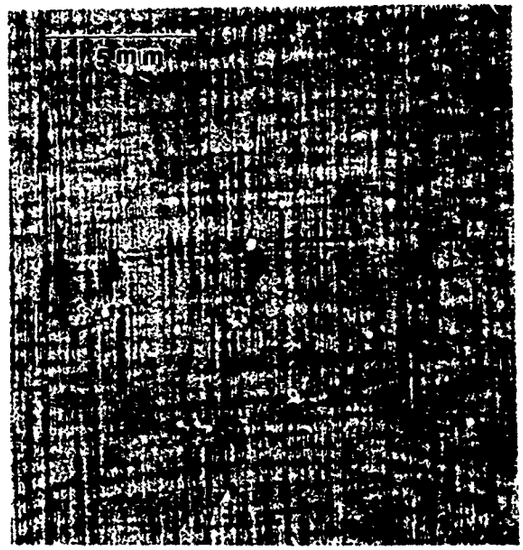

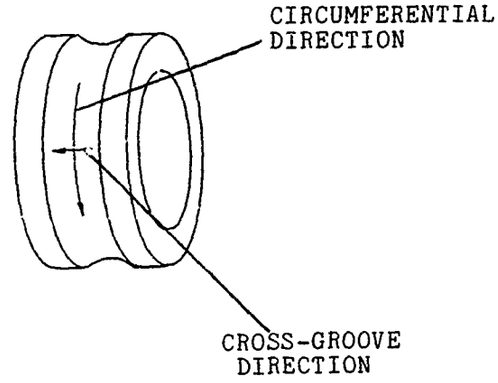

ORIENTATION OF MICROGRAPHS

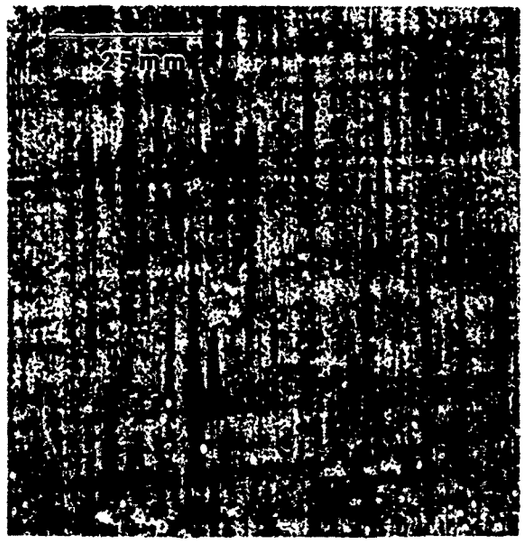

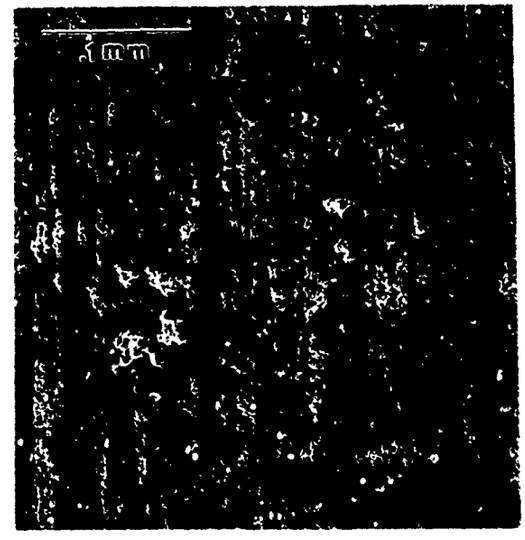

Figure 12. SEM Micrographs Showing Cross-Groove Orientation of Micro-Pits (Arrows) in Ball Path of EB Hardened Inner Ring (Bearing #331-201, Five Hours on Test)

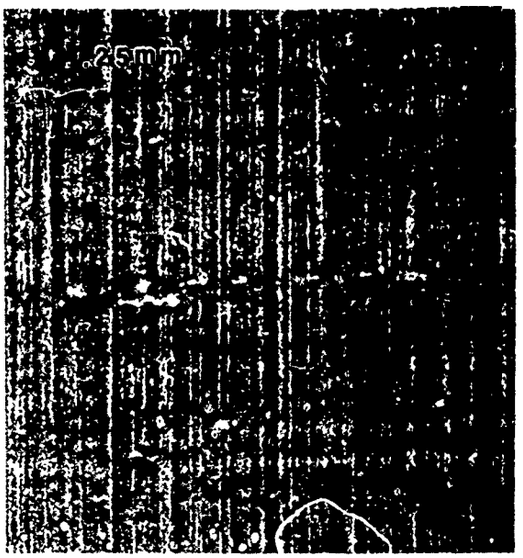

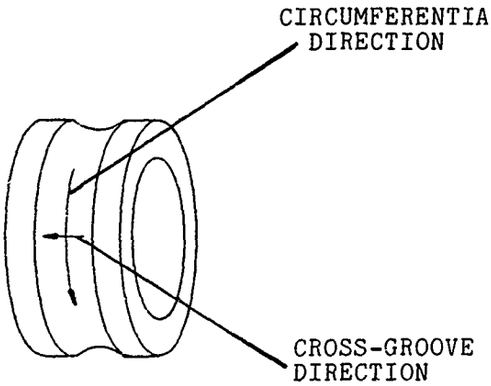

ORIENTATION OF MICROGRAPHS

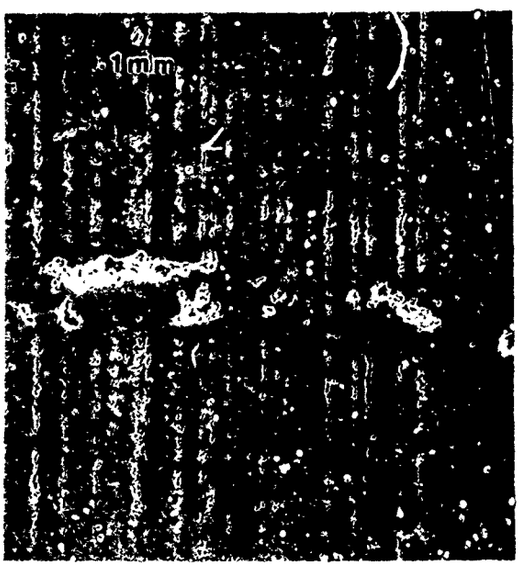

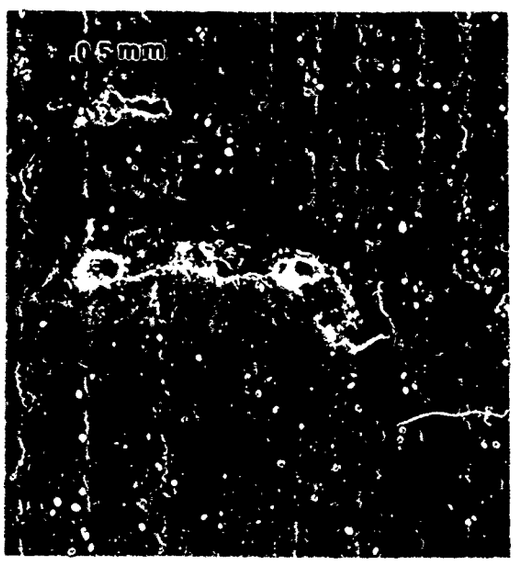

Figure 13. SEM Micrographs Showing Cross-Groove Orientation of Micro-Pits in Ball Path of EB Hardened Inner Ring (Bearing #331-202, Five Hours on Test)

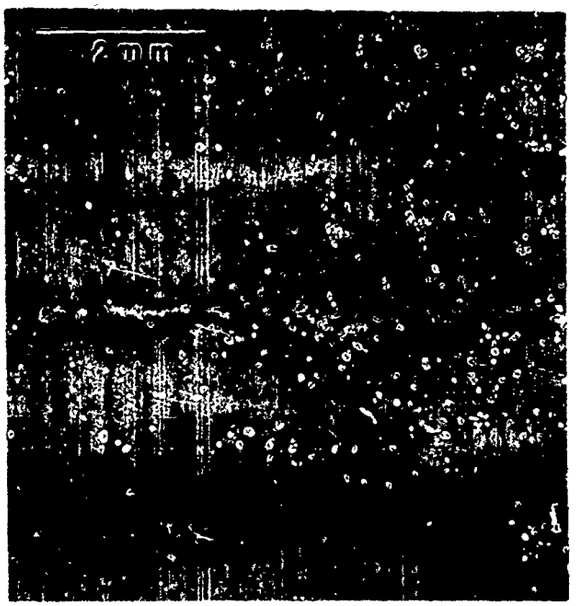

Figure 14. SEM Micrograph Showing Cross-Groove Alignment of Micro-Pits in Center of Ball Path of Unrun EB Hardened Inner Ring. (Nital Etch)

pits were present prior to fatigue testing. The size, frequency and distribution of these indications suggests an association with the characteristic carbide orientation in M50 steel.

The bearing rings in this program were machined from extruded tube. In the manufacture of tube (or bar stock), carbides in the steel are aligned in the direction of extrusion or rolling, i.e. along the axial dimension of the tube. Figure 15(A) shows a schematic representation of the tube from which the inner rings were machined and a photomicrograph of the actual carbide orientation. In Figure 15(B) it is shown that at the bottom of the ball groove, the aligned carbides are oriented in a manner consistent with the pattern of micro-pits shown in Figures 12 and 13.

Further substantiation of the micro-pit/carbide association was obtained through observation of the carbide orientation in conventionally through hardened M50 inner rings. Figure 16 shows the appearance of the cross-groove carbide alignment in a through hardened M50 steel ring made from the same tubing used for the EB processed inner rings. Use of the backscatter mode with the scanning electron microscope highlights the location of the carbides, which appear as the white constituent in Figure 16(B). No indications of the cross-groove pitting was observed in the through hardened rings.

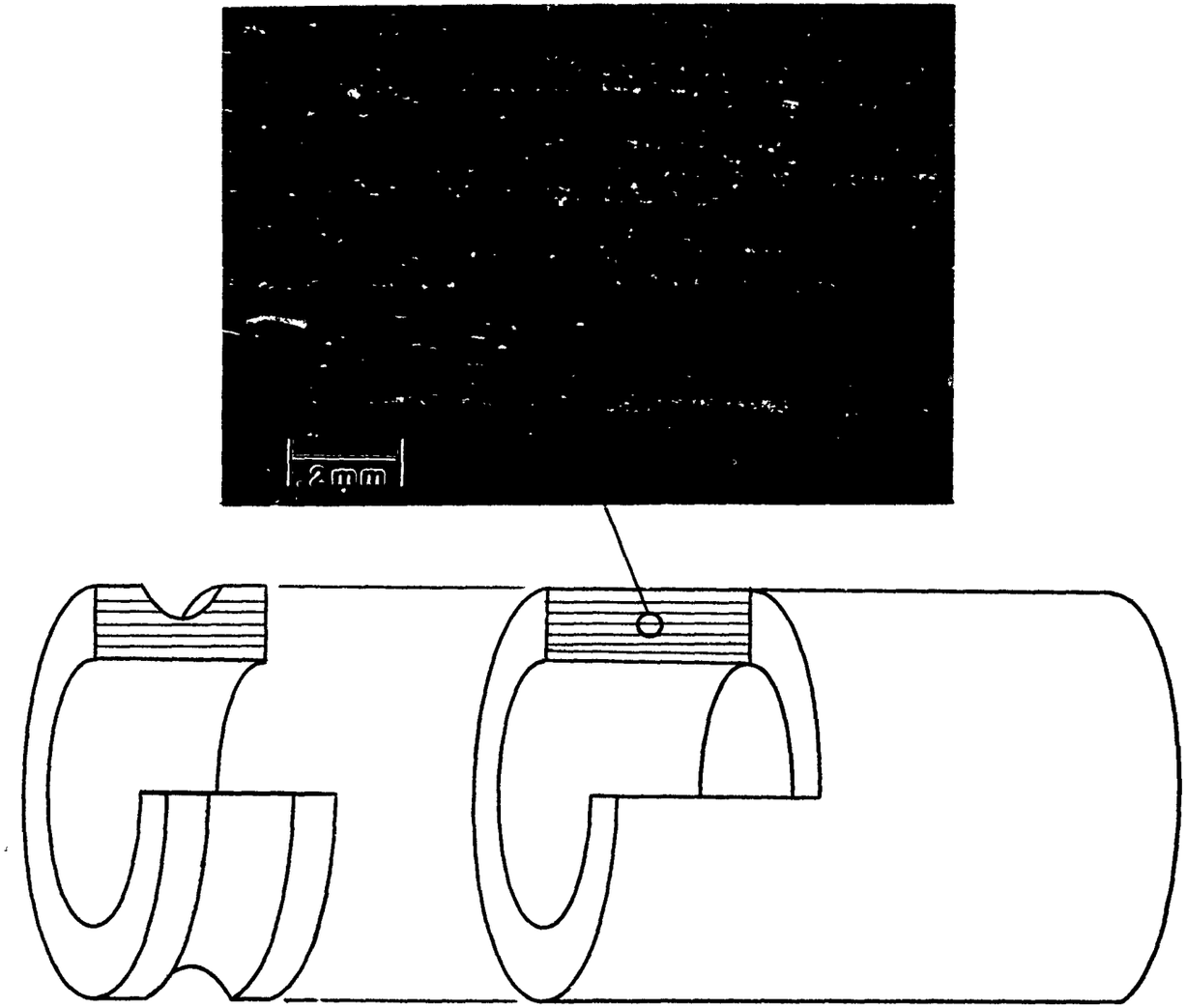

Figure 15(A). Orientation of Carbide Bands in Tube Stock and in Bearing Ring Machined from Such

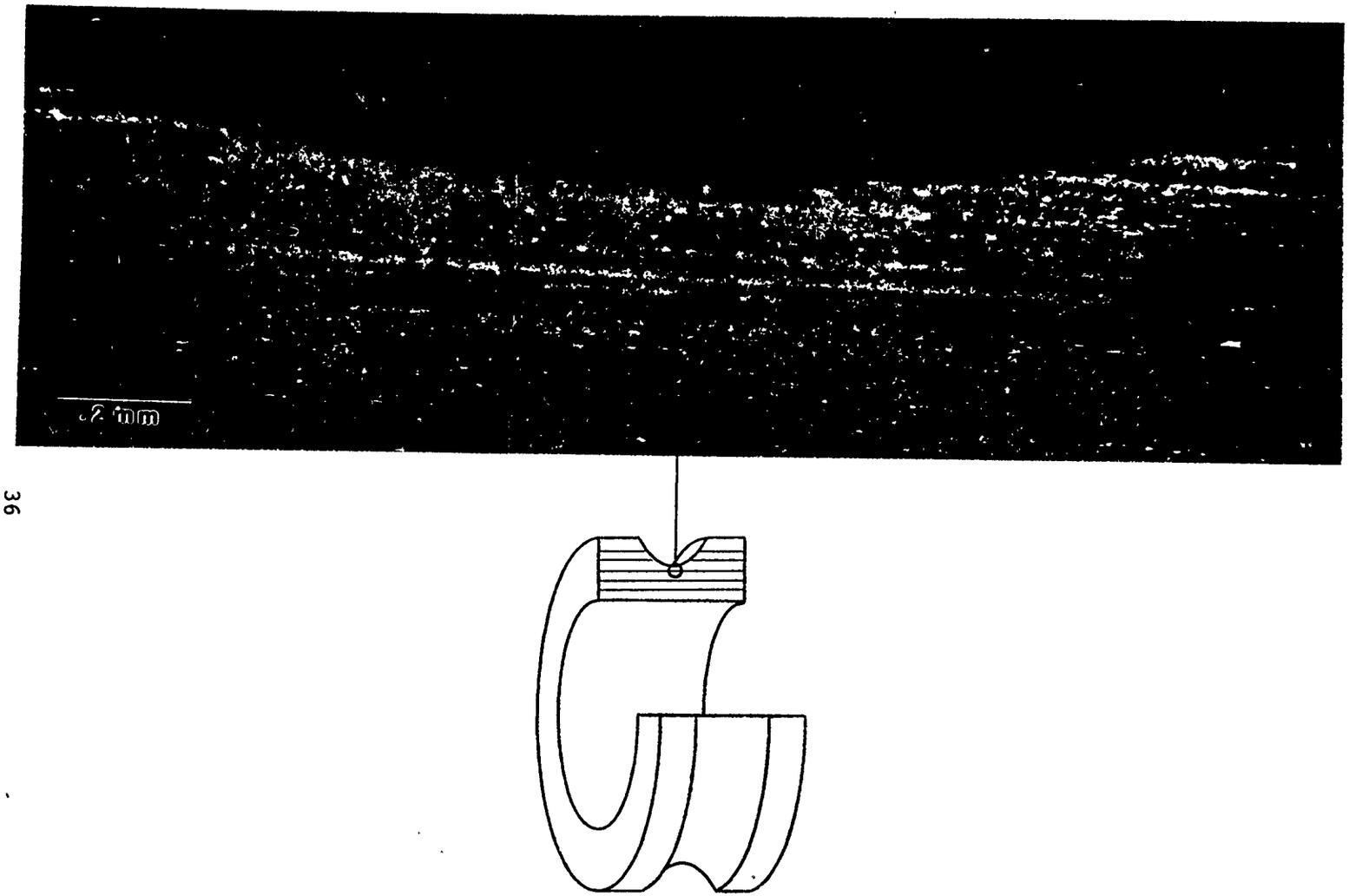

Figure 15(B). Composite Photomicrograph of Carbide Bands in Ball Groove of EB Hardened M50 Steel Inner Rings

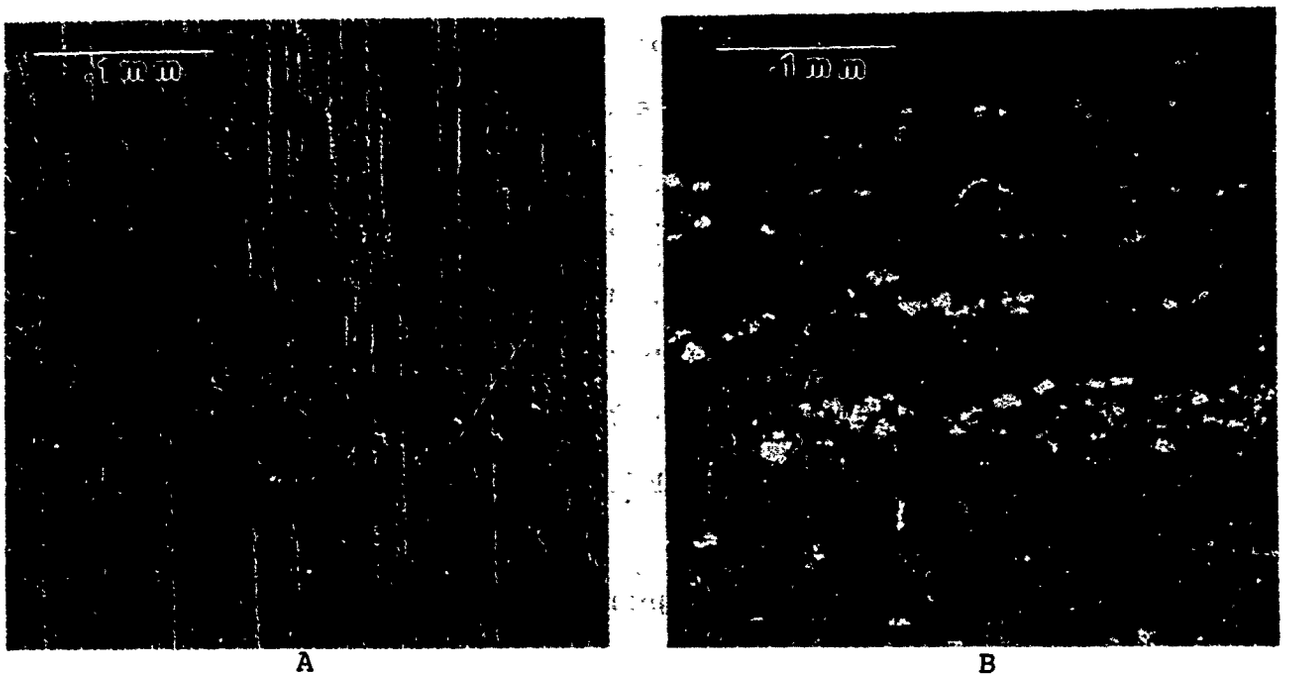

Figure 16. SEM Micrographs Showing Carbide Bands in Ball Groove of Conventionally Through Hardened M50 Steel Inner Ring (A) Secondary Electron Mode (B) Backscatter Mode

Figure 17 contains a photomicrograph of an axial section through an EB surface hardened inner ring. The carbides close to the EB ! ·ated surface have gone partially into solution due to the high surface temperature experienced during EB processing. The matrix material surrounding the carbides is locally enriched with alloying elements in proportion to the amount of carbide taken into solution. The matrix enrichment promoted the local retention of austenite which envelops what remains of the undissolved carbide. A photomicrograph showing the carbide appearance in conventionally through hardened M50 steel is shown in Figure 17 for comparison.

Figure 18 contains high magnification scanning electron micrographs of a metallographically prepared section of an EB hardened inner ring. Carbide dissolution, pits, which appear to be former carbide residences, and grain boundary outlining are apparent. The dark appearance of the grain boundaries in the backscatter images indicate grain boundary separation (i.e. cracking).

It is concluded that the temperatures experienced at the surface and near surface regions during EB processing were excessive for M50 steel. This resulted in an alteration of the microstructure in the vicinity of the primary carbides. During ball groove grinding, these regions separated from the

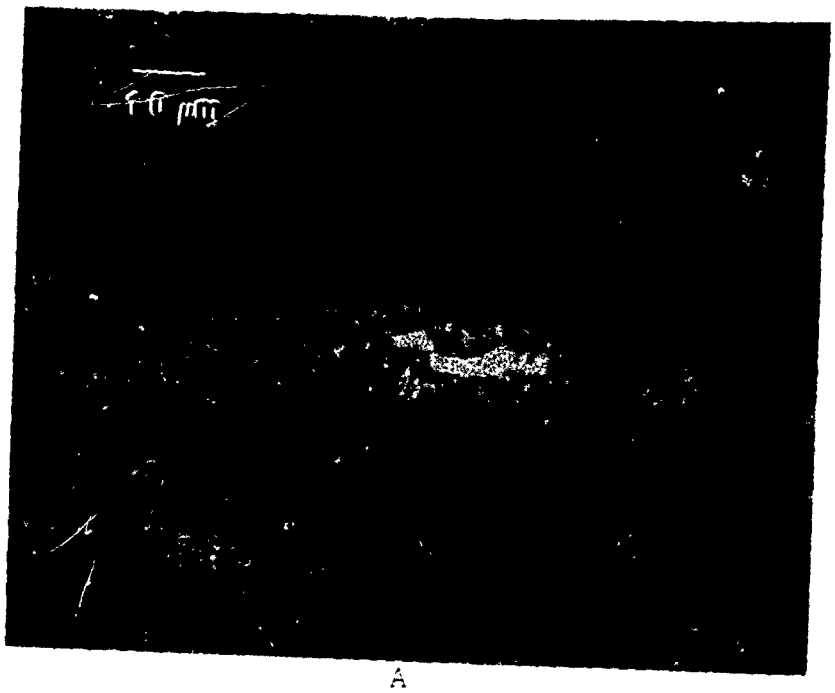

A

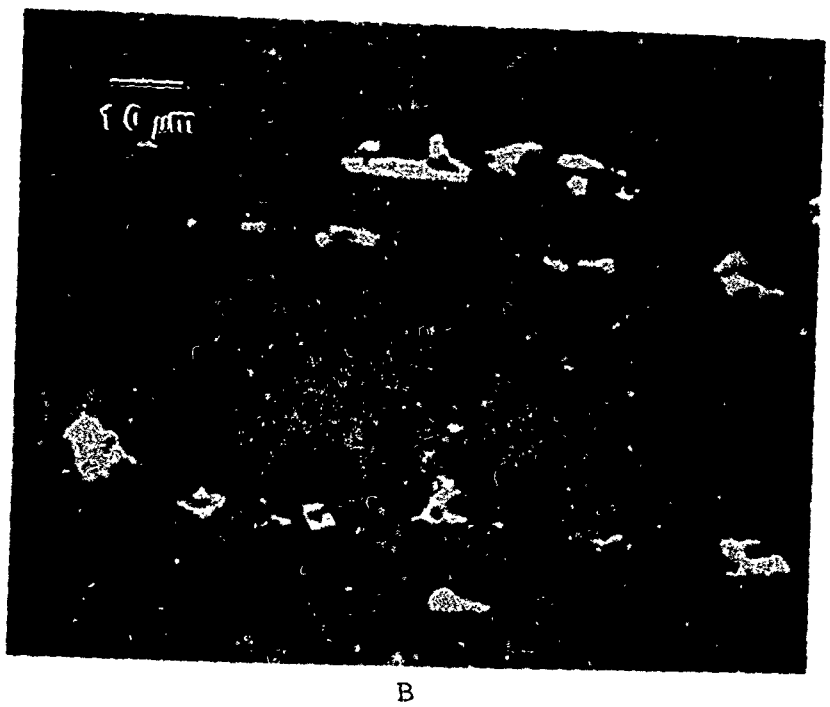

B

Figure 17. Photomicrographs of Carbide Morphology
(A) Near Surface Region of EB Hardened Inner Ring - M50 Steel
(B) Conventional Through Hardened M50 Steel

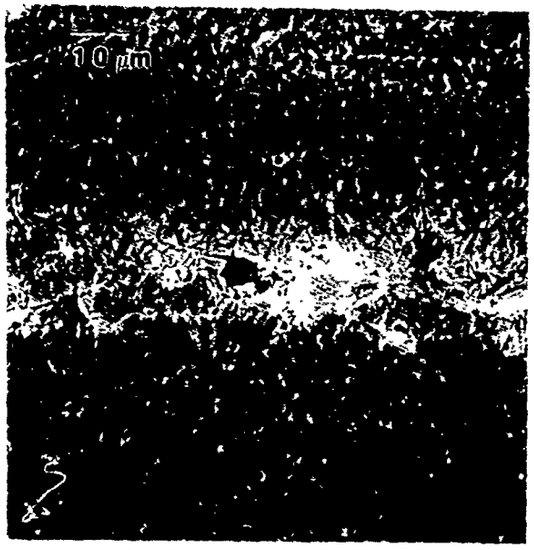

A (Backscatter Mode)

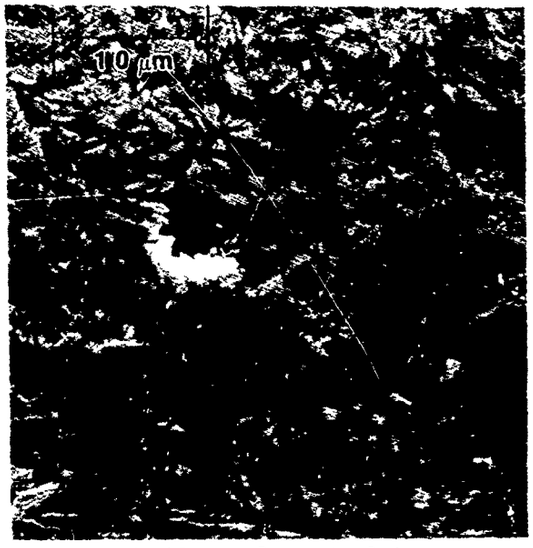

B (Secondary Mode)

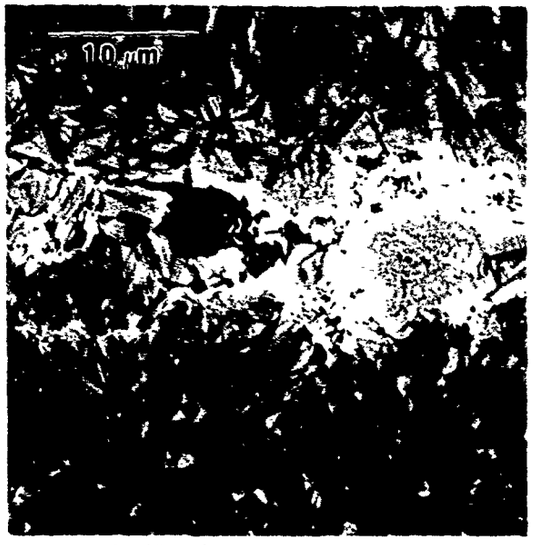

C (Backscatter Mode)

Figure 18. SEM Micrographs Showing Pit (Former Carbide Residence, Dissolved Carbide (White) Areas in A & C) and Apparent Grain Boundary Separation

adjacent matrix leaving the aligned cross-groove pits. These pits represent a severe disruption of the integrity of the rolling contact surface. The extremely short fatigue life experienced is consistent with their presence.

The microstructural alteration giving rise to the pits was confined to a surface region of approximately 0.008-inch (0.2mm) deep. Case depth and hardness profile were both sufficient to permit regrinding of the EB processed rings to remove 0.010 inch (0.25mm) per surface and still provide surface hardness and case depth adequate for life testing (Figure 19). Reworking of the bearings containing the EB processed inner rings was performed under AFWAL Manufacturing Technology Contract F33615-78-C-5018.

After regrinding, the EB surface hardened inner rings provided excellent performance in life testing, with an L_{10} of 151 x 10^6 revolutions. This life is 65% higher than the L_{10} of 91 x 10^6 revolutions obtained with the through hardened baseline group. The difference in the lives obtained by the two methods of hardening is not statistically significant, since the life of the through hardened group is within the confidence limits of 23 x 10^6 and 281 x 10^6 revolutions established for the EB processed group. Therein, however, lies the significance of the test results; i.e. from these test data, there is no statistically significant difference between the rolling contact fatigue

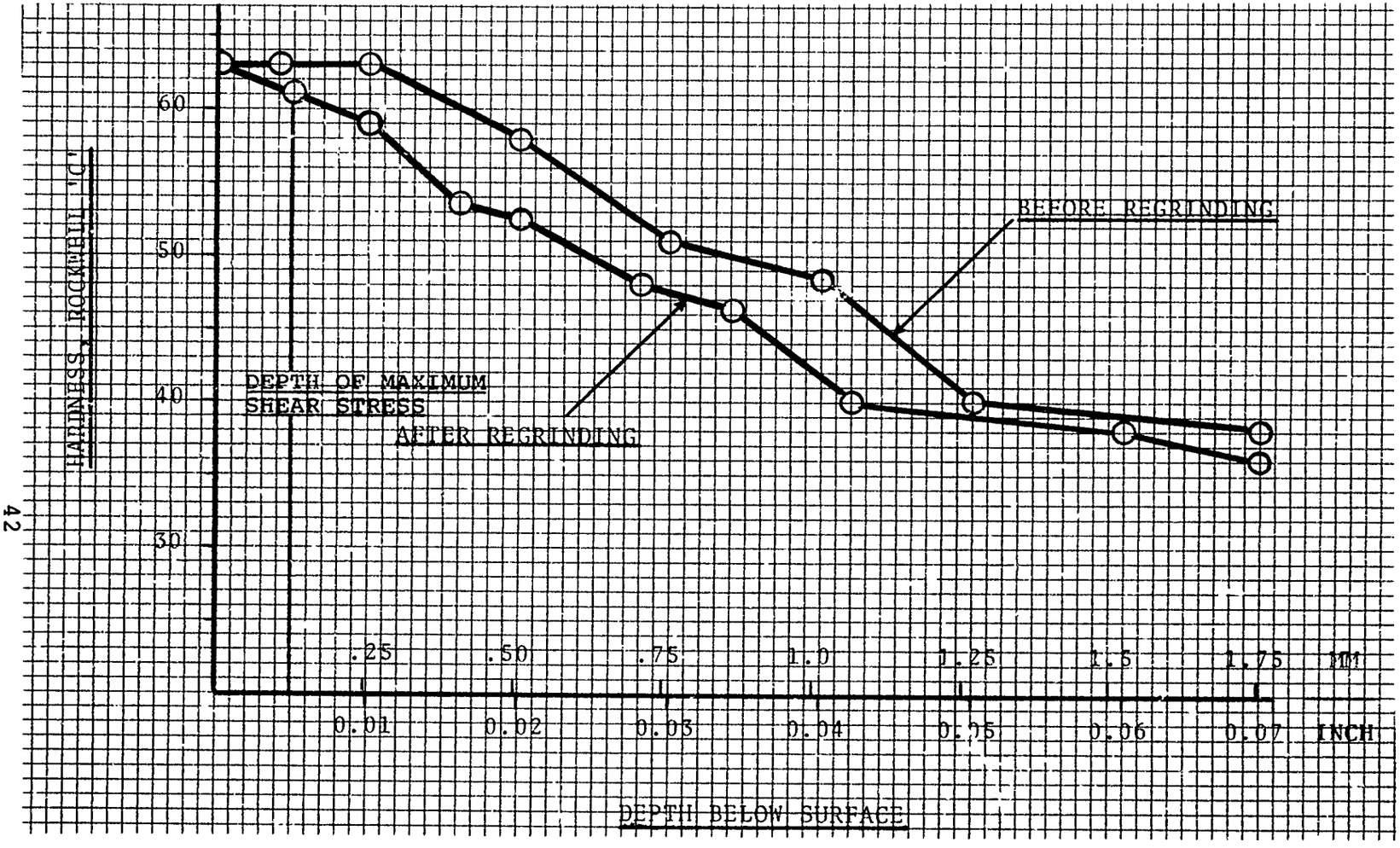

Figure 19. Hardness Profiles in EB Surface Hardened 6009 VCD Inner Rings Before and After Regrinding - M50 Steel

lives of conventionally through hardened and EB surface hardened VIM-VAR M50 steel. The objective of this program was to determine these life relationships and the results indicate that EB surface hardening provides fatigue life at least equal to that of conventional through hardening as applied to VIM-VAR M50 steel.

As described in [5], the EB processing was accomplished by generating a rectangular EB raster pattern covering the width of the 6009 size ball bearing inner ring and a circumferential length of approximately 0.5 inch (12.5mm). The ring was rotated through one revolution under the raster pattern. Beam power was ramped down as the heat path closure point was approached. This was done to preclude localized overheating due to the additive effects of residual and applied thermal energy. The absence of over-tempering in or around the closure region is a manisfestation of the transformation kinetics of M50 steel. They are such as to permit completion of the circumferential heat pass before the first region heated begins to transform. During EB processing each ring was marked on a side face to identify the heat path closure region.

In rolling contact fatigue testing, the first inner ring failure occurred after 137 x 10^6 revolutions. Five additional inner ring failures were accumulated between 154 x 10^6 and 325 x 10^6 revolutions. All inner ring failures are characteristic of classical subsurface initiated rolling contact fatigue spalling.

It is particularly noteworthy that in each of the six failures, spalling initiated within the circumferential region corresponding to the start-stop overlap of the EB heat treat path.

Microstructurally, only subtle variations were observed between the closure region and near surface regions remote from such, and these differences were also observed in unfailed rings that had run in excess of 500 x 10^6 revolutions. It appears that the closure region experienced a slightly higher temperature than the rest of the circumference, giving rise to locally higher retained austenite content within the first few thousandths of an inch of the tested surface. Since both failed and time-up rings exhibit the same appearance, a susceptibility to secondary effects may be indicated rather than an inherent deficiency of the closure region with respect to rolling contact fatigue. For example, subtle variations in surface texture due to grinding, undetected susceptibility to debris denting or localized perturbation of the residual stress state may provide for preferential failure initiation in the closure region. Although the closure region apparently represents a preferred failure initiation site, it is appropriate to recognize that three inner ring failures occurred in the testing of the through hardened baseline group at lives less than that of the first EB processed ring failure. Nevertheless, realization of the full potential of the rolling contact fatigue performance of EB surface hardened M50 steel

will require additional consideration of heat path closure effects.

Radial Expansion of Fatigue Tested Inner Rings

The bearing ring failure mechanism leading to catastrophic fracture in high DN applications is intimately related to centrifugally induced circumferential tensile stress and radial fatigue crack propagation that proceeds under the influence of that circumferential tension. Under such conditions radial crack propagation progresses until a crack length is achieved which is critical with respect to the imposed tensile stress. At that point crack instability ensues resulting in rapid through section fracture and destruction of the bearing ring. In [1], the dramatic consequences of such a failure are illustrated by the total destruction of the inner ring through fragmentary fracture.

The radial expansion tests described herein were not intended to simulate high DN bearing ring failure: to do so requires simultaneous, rather than consecutive, application of rolling contact stressing and tensile hoop stress. The intent was to determine, under exaggerated hoop stress conditions, the relative fracture behavior of through hardened and EB surface hardened M50 steel inner rings.

The most pronounced difference in fracture behavior between the through hardened and EB surface hardened rings is the absence

of fragmentation with the surface hardened rings. Figures 6 and 8 shows representative examples of through hardened and EB surface hardened rings after fracture at comparable diametral expansions. The through hardened rings fractured into several pieces, the EB processed rings exhibit a single through-section fracture. With the through hardened rings, fragmentation occurred in a region 180 degrees from the primary fracture, apparently the result of impact type loading from the rapid release of elastic strain energy associated with the initial fracture. The absence of secondary fracture with the surface hardened rings is attributable to a combination of factors. Yielding of the lower hardness core material most likely occurred prior to fracture, thereby reducing the magnitude of elastic strain energy released at fracture. Also, more strain energy would be consumed in the initial fracture due to the higher toughness core material. Additionally, the low hardness core material is much more resistant to impact failure than fully hardened M50 steel, making secondary fracture more unlikely.

Expansion of an EB processed ring that was not spalled (#253) produced fracture which initiated at a ball path-land juncture (Figure 9A). There were no observations indicating subsurface failure initiation associated differential case-core plasticity.

Fracture of the spalled EB processed ring (#247) that was expanded initiated in the spalled region at the bottom of the ball path (Figure 9C). Otherwise, the fracture surface characteristics appear the same as those of the unspalled EB processed ring.

The spalled and unspalled EB hardened rings fractured at diametral expansions of 0.0194 and 0.0192 inch (493 and 488 microns) respectively. Hoop stress values calculated assuming elastic behavior are invalid, since yielding of the core material probably occurred. The yield strength of M50 steel tempered to RC35 is of the order of 175 ksi (1206 MPa). An elastically deformed ring at the indicated range of diametral expansion would experience a hoop stress of approximately 275 ksi (1896 MPa).

Through hardened rings without spalls sustained diametral expansion prior to fracture from a minimum of 0.0221 inch (561 microns), to 0.0252 inch (640 microns). Four rings in the middle of this expansion range did not fracture. Although there were no indications of surface spalling in these rings, it is suspected that the range of diametral expansion, the associated range of hoop stress, and whether or not fracture occurred at a particular stress level, are indications of subsurface conditions associated with various stages of incipient rolling contact fatigue failure.

The range of calculated hoop stress experienced by the unspalled through hardened rings is from 317 to 362 ksi (2186 to 2496 MPa). With the exception of ring No. 109 (corresponding

to the 317 ksi (2186 MPa) fracture) all fractures occurred within the range of reported uniaxial tensile properties for M50 steel at a hardness of RC61.5; i.e. 0.2% yield stress = 330 ksi (2275 MPa), fracture stress = 380 ksi (2620 MPa) [6,7].

Through hardened rings with spalled surfaces all fractured through the spalled region at the apparent location of spall initiation (Figure 7). The range of diametral expansion is 0.0129 to 0.0221 inch (330 to 561 microns). The corresponding range of calculated hoop stress is 187 to 317 ksi (1289 to 2186 MPa). The lower stresses required to produce fracture of the spalled rings is attributed to the stress concentrating effect and pre-existent cracks associated with the raceway spalls.

The SEM micrographs of Figure 20 show the typical appearance of all through hardened ring fracture surfaces. Quasi-cleavage facets, tear ridges and voids associated with both carbides and void coalesence are depicted. These features are consistent with M50 fracture surfaces described in [6].

The fracture surfaces of EB processed rings exhibit predominant indications of a ductile fracture mode in the core region. Fracture in the case, in a region corresponding to a hardness of RC60 to 62, is a mixture of cleavage and more pronounced indications of ductile fracture than observed with the through hardened M50 steel (Figure 21).

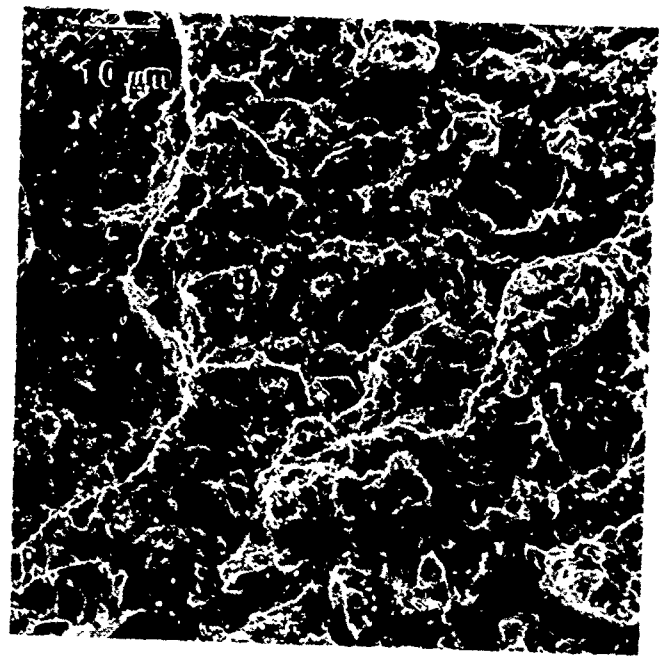

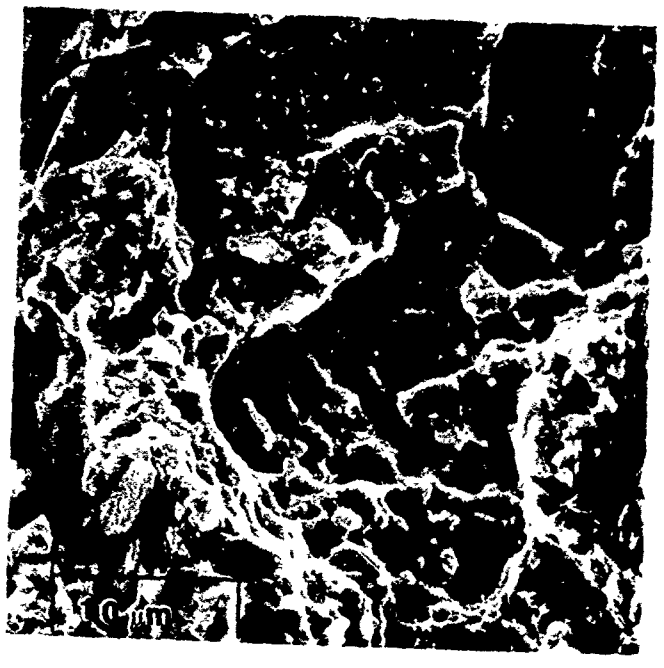

Figure 20. Fracture Surface of Radially Expanded Through Hardened M50 Steel Inner Ring

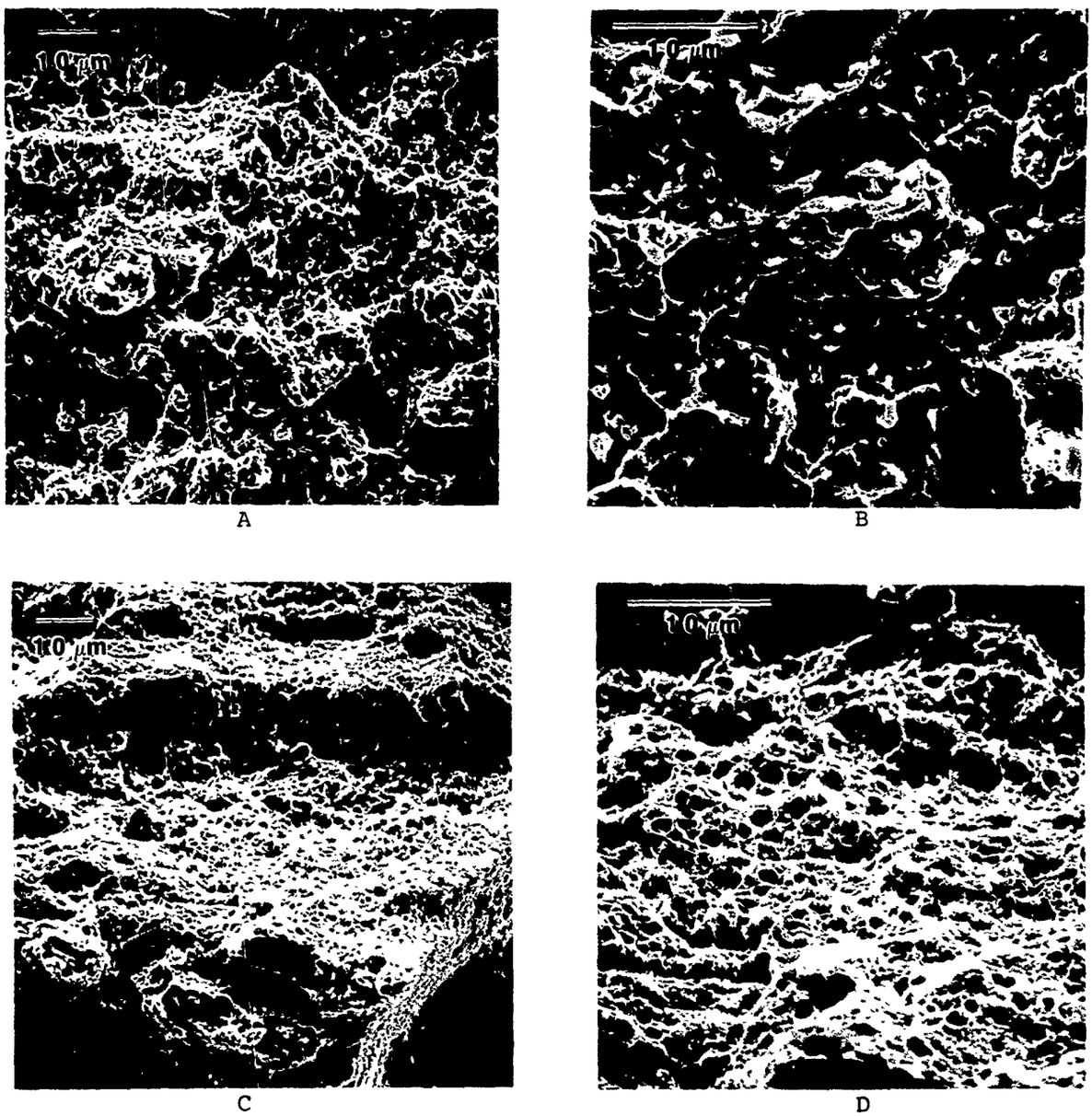

Figure 21. Fracture Surface of Radially Expanded EB Surface Hardened M50 Steel Inner Ring. A & B - Case at RC61, C & D - Core at RC35

Concluding Remarks

The hoop stress level required to produce rapid fracture in conjunction with a spall (in the absence of rolling contact stressing) is clearly in excess of that associated with any conceivable bearing application environment. However, bearing ring fracture has been experienced with service level hoop stresses well below 40 ksi (275 MPa) when combined with rolling contact stressing. Such occurrences highlight the significance of the relationship between hoop stress and fatigue crack propagation in rolling contact.

Quantitative assessment of the effects of tensile hoop stress on crack initiation/propagation in rolling contact has not been reported in the literature. However, the indicated trend is that early failure, and under some conditions, catastrophic failure, is promoted [2,8]. High hoop stress levels not only promote early failure initiation, but through-section fracture with no clear indications of prior spalling [8]. Low to intermediate stress levels have provided mixed modes of failure wherein ring fracture may or may not be associated with surface spalling [2].

Although the complex interactive effects of the Hertzian stress field, applied hoop stress and residual stress have not been characterized, the observed effect of net tensile hoop stress is accelerated radial fatigue crack propagation. This

phenomenon has been observed in heavy section commercial bearing applications as well as in thin section aircraft bearings and is intimately associated with tensile hoop stress.

The need for improved subsurface fatigue crack propagation resistance dictates the requirement for a core region of relatively low hardness. The essentiality of maintaining rolling contact life consistent with existing turbine mainshaft bearing performance provides strong incentive for continued use of the service proven VIM-VAR M50 steel. The results of the rolling contact fatigue testing of EB surface hardened VIM-VAR M50 steel demonstrates that both a low hardness core and fatigue life at least equal to conventionally heat treated M50 steel are attainable.

In the absence of a comprehensive analysis of the interactive effects of hoop stress and rolling contact stressing, and fatigue crack propagation data generated under the conditions corresponding to the output of such, a priori conclusions pertaining to the magnitude of fracture resistance improvement associated with EB surface hardening can only be speculative. Therefore, under the existing Manufacturing Technology program (Air Force Contract F33615-78-C-5018), mainshaft size bearing rings (120 mm bore) made of VIM-VAR M50 steel will be EB surface hardened, assembled into bearings, and tested under conditions simulating 3.5×10^6 DN bearing operation in a separate Aero Propulsion Laboratory program

(Air Force Contract F33615-80-C-2018). The test conditions will be demonstrated to produce through section fracture of conventionally through hardened M50 steel rings, thereby providing a basis of comparison for the performance of the EB surface hardened rings.

CONCLUSIONS

1. The VIM-VAR M50 steel used for inner ring manufacture when conventionally through hardened, exhibits an L_{10} life consistent with adjusted rating life calculations using a material factor (a_2) of 5, and a_1 and a_3 factors corresponding to 90 percent reliability and the appropriate operating conditions, respectively. (Adjusted inner ring rating $L_{10} = 62 \times 10^6$ revolutions. Experimental inner ring $L_{10} = 91 \times 10^6$ revolutions.)

2. The rolling contact fatigue life of $L_{10} = 151 \times 10^6$ revolutions obtained with the EB surface hardened VIM-VAR M50 steel rings demonstrates performance that is at least comparable to that of the through hardened VIM-VAR M50 steel.

3. Optimization of the time-temperature relationships in the EB hardening of VIM-VAR M50 steel is required to eliminate life limiting microstructural alterations in the near surface region. Although it has been demonstrated that this surface condition can be successfully accommodated by increased grinding stock allowances, elimination of such would provide for greater processing efficiency.

4. All of the spalling failures in the EB surface hardened rings initiated in the start-stop closure of the EB heating pass. In comparison with the baseline data these failures are not premature, however, closure region performance was the determining factor in the life tests of the EB processed rings. Procedural techniques are available for diminishing heat pass closure effects, and these will be pursued in the manufacture of the bearing rings scheduled for simulated 3.5×10^6 DN testing.

REFERENCES

1. Bamberger, E. N., Zaretsky, E. V. and Singer, H., "Endurance and Failure Characteristic of Main-Shaft Jet Engine Bearing at $3x10^6$ DN," Trans. ASME, J. of Lubrication Technology, October 1976, pp. 580-585.
2. Clark, J. C., "Fracture Failure Modes in Lightweight Bearings," AIAA Journal, Aircraft, Vol. 12, No. 4, April 1975, pp. 383-387.
3. McCool, J. I., "Inference on Weibull Percentiles and Shape Parameter from Maximum Likelihood Estimates," IEEE Trans. on Reliability, Vol. R-19, No. 1, 1970, pp. 2-9.
4. Nelson, W., "Theory and Applications of Hazard Plotting for Censored Failure Data," Technometrics, Vol. 14, No. 4, 1972, pp. 945-966.
5. Maurer, R. E., "High Energy Beam Heat Treatment of Bearing Races," Fourth Interim Report, IR-232-8-IV, Air Force Contract F33615-78-C-5018, September 1980.
6. Rescalvo, J. A., "Fracture and Fatigue Crack Growth in 52100, M50 and 18-4-1 Bearing Steels," Doctoral Thesis, Dept. of Materials Science and Engineering, MIT, submitted May 4, 1979.
7. Technical Data Sheet - M50 High-Speed Steel - Carpenter Technology Corporation, Reading, PA.
8. Kepple, R. K. and Mattson, R. L., "Rolling Element Fatigue and Macroresidual Stress," Trans. ASME, Journal of Lubrication Technology, Series F, Vol. 92, January 1970, pp. 76-82.

APPENDIX A

CALCULATION OF

6009 VCC INNER RING ADJUSTED RATING LIFE

1. Determination of Inner Ring Dynamic Capacity

The L_{10} value of the inner ring is determined from the relationship of:

$$C = g_c \, C_i \qquad (1)$$

where:

C = Dynamic capacity of the whole bearing

C_i = Dynamic capacity of the inner ring only

g_c = is a function of the material and internal bearing parameters.

In the case of 90% reliability and using the maximum inner ring and outer ring ball groove radii for the tolerance employed, i.e. $r_{i_{max.}} = r_{e_{max}} = 4.547$ mm.

$$g_c = \left[1 + \left(\frac{C_i}{C_e}\right)^{10/3}\right]^{-0.3}$$

where $$\frac{C_j}{C_e} = f_3 \left[\frac{r_i}{r_e} \frac{2r_e - Da}{2r_i - Da}\right]^{0.41}$$

and $$f_3 = 1.04 f_4$$

and $$f_4 = \left[\frac{1 - \gamma}{1 + \gamma}\right]^{1.72}$$

and $$\gamma = \frac{Da \cos \alpha}{d_m}$$

where D_a = Ball diameter mm = 8.73mm

α = Contact angle = 0^o

d_m = Bearing pitch diameter = 60mm

$$\gamma = \frac{8.73 \cos 0^o}{60} = 0.1455$$

$$f_4 = \left[\frac{1 - 0.1455}{1 + 0.1455}\right]^{1.72} = 0.604$$

$$f_3 = 1.04\ (0.604) = 0.628$$

$$\frac{c_i}{c_e} = 0.628\ \frac{4.547}{4.547}\ X\ \left[\frac{2(4.547) - 8.73}{2(4.547) - 8.73}\right]^{0.41} = 0.628$$

$$g_c = [1 + (0.628)^{10/3}]^{-0.3} = 0.9439$$

$$c_i = C/g_c = 3630/0.9439 = \underline{3845\ \text{lbs}}\ \text{or}\ \underline{17.103\ \text{kN}}$$

2. Determination of Inner Ring Adjusted Rating Life

Material: VIM/VAR AISI M50 Steel

Test Conditions:

Speed - 9700 rpm

Radial Load - 7.495 kN (1685 lbf)

Lubricant - MIL-L-7808G

Bearing Operating Temperature - 333K (60°C)(150°F)

Based upon the SKF Engineering Manual fatigue life formula for the determination of basic rating life of a deep groove ball bearing, the basic rating life of an inner ring is:

$$L_{10_i} = \left(\frac{C_i}{P}\right)^3$$

where C_i = Inner ring basic dynamic load rating

P = Equivalent dynamic bearing load.

In the case of 6009 VCC deep groove ball bearing for a C_i value of 17.103 kN and an equivalent applied load of 7.495 kN:

$$L_{10_i} = 11.88 \times 10^6 \text{ revolutions}$$

However, considering the improved materials and the lubricant employed, the adjusted basic rating life is:

$$L'_{n_i} = a_1 a_2 a_3 \; L_{10}$$

where L'_{n_i} = Adjusted inner ring rating life in millions of revolutions.

L_{10_i} = Basic inner ring rating life in millions of revolutions.

a_1 = Reliability factor (which for 90% reliability = 1)

a_2 = Material factor (which for VIM/VAR AISI M50 steel is 5 from SKF Report AL79T027)

a_3 = Operating conditions factor (from ASME "Life Adjustment Factors for Ball & Roller Bearings" Figure 2 is 1.05

Therefore $L'_{n_i} = (1)(5)(1.05)(11.88 \times 10^6) = \underline{62 \times 10^6 \text{ revolutions}}$

APPENDIX B

DETERMINATION OF EFFECTIVE OUTER SURFACE RADIUS FOR HOOP STRESS DETERMINATION - 6009 INNER RINGS

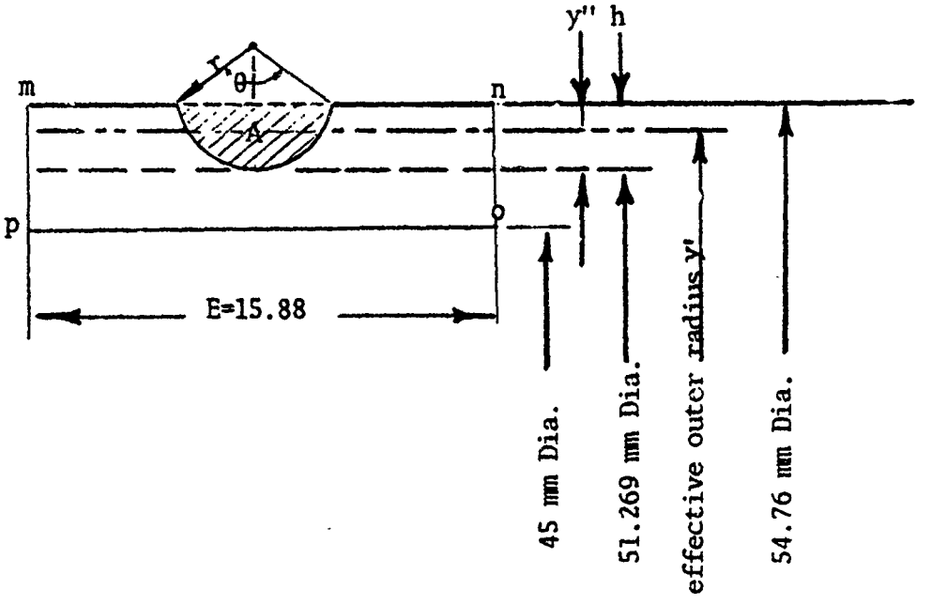

$$r = 4.52 \text{ mm}$$

$$h = \frac{54.75-51.269}{2} = 1.741 \text{ mm}$$

Area $A = \frac{r^2}{2}(\theta - \sin\theta)$ (Eshbach)

$$1/2\,\theta = \cos^{-1}\frac{r-h}{r} = \cos^{-1}\frac{4.52-1.741}{4.52} = 52.06^\circ$$

$$\theta = 104.12^\circ \qquad \theta_{\text{radians}} = 1.8173$$

$$A = \frac{4.52^2}{2}(1.8173-\text{Sin } 104.12^\circ) = 8.66 \text{ mm}^2$$

Area Section mnop - Area A = hE - Area A

$$1.741(15.88)-8.66 = 18.99 \text{ mm}^2$$

$$\text{Effective radius } y' = \frac{51.269}{2} + y'' = 25.635 + \frac{18.99}{15.88} = 26.83 \text{ mm}$$

DETERMINATION OF HOOP STRESS - 6009 INNER RINGS

$$\sigma_t = \frac{P(b^2 + c^2)}{c^2 - b^2}$$

$$P = \frac{E\delta}{2b}\left[1-\left(\frac{b}{c}\right)^2\right]$$

where σ_t = Hoop stress

b = Inner ring internal radius = 22.50 mm

c = Inner ring "effective" outer radius = 26.83 mm

E = Modulus of steel = 206 X 10^3 N/mm^2

δ = 1/2 diametral expansion of inner ring at failure in mm

$$P = \frac{206 \times 10^3\delta}{2(22.50)}\left[1-\left(\frac{22.50}{26.83}\right)^2\right] = 1.358 \times 10^3\delta$$

$$\sigma_t = \frac{1.358 \times 10^3\delta\ (22.50^2 + 26.83^2)}{26.83^2 - 22.50^2} = \frac{1.6652 \times 10^6\delta}{2.1356 \times 10^2}$$

$$\sigma_t = 7.797 \times 10^3\delta \text{ N/mm}^2$$

*U.S.Government Printing Office: 1982 — 559-003/2028